Bioorganic & Medicinal Chemistry 16 (2008) 8447–8465

Contents lists available at ScienceDirect

Bioorganic & Medicinal Chemistry

journal homepage: www.elsevier.com/locate/bmc

Antimicrobial and cytotoxic arylazoenamines. Part III: Antiviral activity of selected classes of arylazoenamines ☆

Michele Tonelli [a], Vito Boido [a], Caterina Canu [a], Anna Sparatore [b], Fabio Sparatore [a,*], Maria Silvia Paneni [c], Maurizio Fermeglia [c], Sabrina Pricl [c], Paolo La Colla [d], Laura Casula [d], Cristina Ibba [d], David Collu [d], Roberta Loddo [d]

[a] *Dipartimento di Scienze Farmaceutiche, Università di Genova, Viale Benedetto XV 3, 16132 Genova, Italy*
[b] *Istituto di Chimica Farmaceutica, Università di Milano, Viale Abruzzi 42, 20131 Milano, Italy*
[c] *Dipartimento di Ingegneria Chimica, dell'Ambiente e delle Materie prime, Università di Trieste, Via Valerio 10, 34127 Trieste, Italy*
[d] *Dipartimento di Scienze e Tecnologie Biomediche, Università di Cagliari, Cittadella Universitaria, S.S. 554, Km 4.500, 09042 Monserrato, Cagliari, Italy*

ARTICLE INFO

Article history:
Received 19 May 2008
Accepted 13 August 2008
Available online 15 August 2008

Keywords:
Arylazoenamino compounds
Antiviral activity
RNA and DNA viruses
Pharmacophore models

ABSTRACT

Eighty-five arylazoenamines, characterized by different types of aryl and basic moieties, have been synthesized and evaluated in cell-based assays for cytotoxicity and antiviral activity against a panel of ten RNA and DNA viruses.

The most commonly affected viruses were, in decreasing order, CVB-2, RSV, BVDV, YFV, and Sb-1; the remaining viruses were either not affected (HIV-1, VSV, and VV) or susceptible only to a very few compounds (Reo-1 and HSV-1).

Thirty-five compounds exhibited high activity, with EC_{50} in the range 0.8–10 μM, and other 28 compounds had EC_{50} between 11 and 30 μM, thus indicating that the arylazoenamine molecular pattern is an interesting novel pharmacophore for antiviral agents against ssRNA viruses. Moreover, some compounds (as **28**, **32**, **42**, and **53**) appear of high interest, being devoid of toxicity on the human MT-4 cells (CC_{50} > 100 μM).

A ligand-based computational approach was employed to identify highly predictive pharmacophore models for the most frequently affected viruses CVB-2, RSV, and BVDV. These models should allow the design of second generation of more potent inhibitors of these human and veterinary pathogens.

1. Introduction

Since 20 years, we have shown that by reacting α-(*tert*-amino)-ketones with excess of arylhydrazines, in the presence of acids, stable, red-orange arylazoenamines are formed, instead of (or in addition to) the expected indoles.[1,2]

It was assumed that the essential step for the formation of this kind of compounds is the tautomerization of the initially formed arylhydrazone into the corresponding arylhydrazoenamine, which is then oxidized by the excess of arylhydrazine, with simultaneous formation of an arylamine and ammonia (Scheme 1).

Arylazoenamino compounds have been already obtained in the past through different pathways, as by reacting arylhydrazines with 2-(bromomethyl)-1-methylquinolinium bromide, or with 1,2,3,3-tetramethylindoleninium iodide,[3] by coupling diazonium salts with the so-called methylene bases as 2-methylene-1,3,3-trimethylindoline,[4] as well as by reacting glyoxal monophenylhydrazone with secondary amine (piperidine[5] and pyrrolidine[6]). Moreover, unstable arylazoenamines were supposed to be formed, at first, in the reaction of diazonium salts with unsaturated amines, that, finally, gives rise to β-phenylhydrazones of substituted glyoxals.[7]

To the best of our knowledge, biological activities of arylazoenamines resulted unexplored until 1990,[8,9] though they can be considered either as sub-structures of *ortho* (and *para*) aminoazo compounds, or as vinylogues of aryltriazenes (either linear or cyclic), many of which are endowed with either antimicrobial, antiparasitic or cytotoxic activities (Fig. 1).

Representative compounds of the first type are the following: 2,6-diamino-3-phenylazo pyridine (pyridium), once used as urinary antiseptic and analgesic; 5-(4-amino-1-naphthylazo)uracil, highly effective against *Schistosoma mansonii*[10,11]; 1-[3-(4-phenylazo-5,6,7,8-tetrahydronaphth-1-yl)amino]-propylpiperidines[12] and 1-[3-(4-phenylazo-5,6,7,8-tetrahydronaphth-1-yl)aminolupinane[13] very active against *Mycobacterium tuberculosis*; and Congo Red, recently shown to be able to inhibit the deposition of prion protein in amyloid plaques.[14,15]

☆ For notes I and II, see Refs. 8 and 9.

* Corresponding author. Tel.: +39 010 512721; fax: +39 010 3538358.
E-mail address: sparator@unige.it (F. Sparatore).

0968-0896/$ - see front matter © 2008 Elsevier Ltd. All rights reserved.
doi:10.1016/j.bmc.2008.08.028

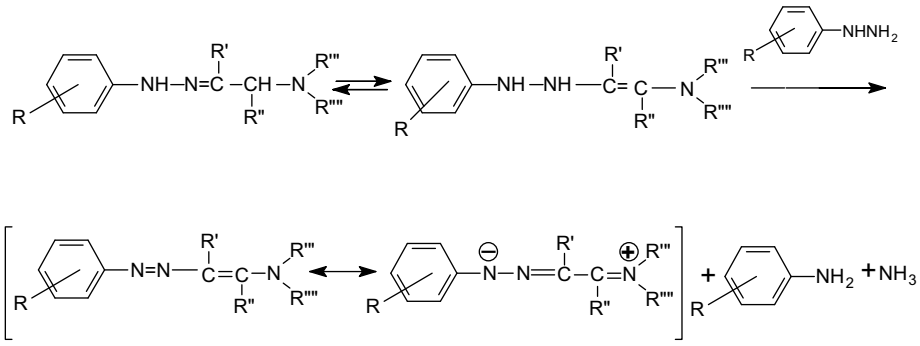

Scheme 1.

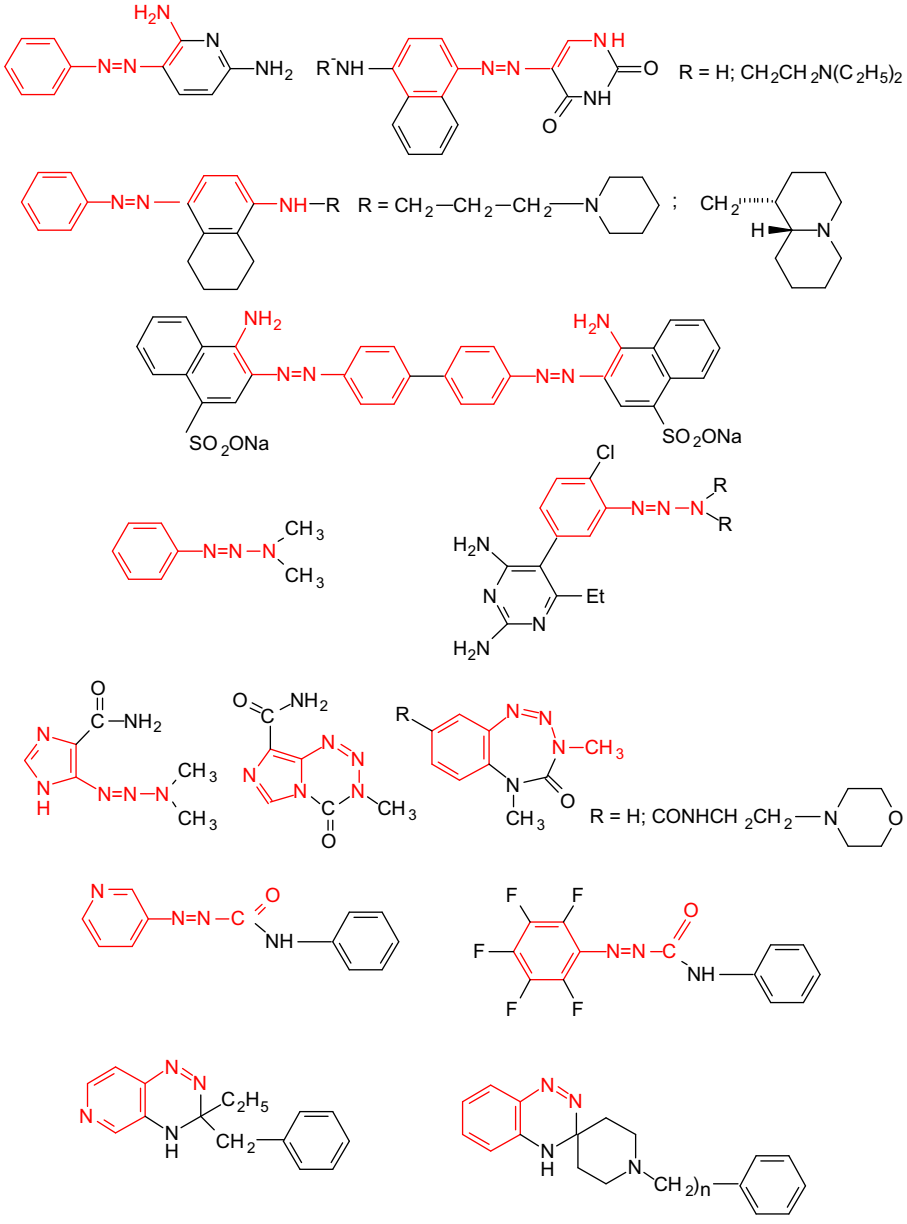

Figure 1. Some biologically active azocompounds reminding arylazoenamines.

Triazenes as a class of compounds[16] hold an important position as carcinogens and/or anticancer agents: 3,3-dimethyl-1-phenyltriazene and, even better, dacarbazine[17] are able to methylate DNA, thus the former resulted in a powerful carcinogen, while the latter is in clinical use for the treatment of malignant melanoma and Hodgkin's disease. A structurally more complex triazene

combines antitumor potential with inhibition of *Pneumocystis carinii*.[18] Temozolamide,[19] closely related to dacarbazine, is currently used to treat malignant glyomas. A recent development of this cyclic acyltriazene is represented by the synthesis of benzotetrazepinones,[20–24] that are very promising agents against breast cancer. It is worth noting that these compounds are weak alkylating agents and may damage DNA by a novel mechanism.

Arylazoenamines could be also seen as simple azocompounds, whose reactivity is somewhat enhanced by the conjugation with the ene double bond, and as such they could be related to the even more activated acyldiazenes. Simple aromatic azocompounds and acyldiazenes are endowed with a variety of biological activities[25,26] (mainly antifungal and cytotoxic), generally related to their ability to oxidize biological thiols, though other mechanisms should be supposed in some cases. Antifungal[27] and antiproliferative[28] activities have been found in a peculiar class of cyclic azocompounds (3,3-disubstituted-3,4-dihydro-1,2,4-benzotriazines[29]), which moreover can display several other pharmacological activities depending on the substituents that are present on the bicyclic system.[30,31]

On this base, some years ago, thirty arylazoenamines were prepared and tested[8,9] for antimicrobial activity against eight Gram+ and Gram− bacterial strains and against eight yeast like fungi. While the antibacterial activity was very poor [MIC in the range from 1 to 2 mg/ml (norfloxacine: MIC = 4–8 μg/ml) and only two occasional values of 512 μg/ml against *Pseudomonas aeruginosa*], a moderate antifungal activity was displayed by most compounds, with MIC from 32 to 512 μg/ml against the whole set of tested fungi (miconazole nitrate: MIC = 0.25–2 μg/ml).

Moreover, a few of these compounds, which were additionally tested against bovine viral diarrhoea virus (BVDV) and coxackie virus type B2 (CVB-2), exhibited an interesting antiviral activity.

Therefore many new arylazoenamines have now been synthesized, and together with part of the previously described compounds were evaluated in cell-based assays for cytotoxicity and antiviral activity against a large panel of RNA and DNA viruses.

On the whole, 85 arylazoenamines have been considered, which may be allotted in seven groups (**A**–**G**) in relation to the nature of the basic moiety (Fig. 2).

Twenty-nine out of these compounds have been already described: nine of structure **A**,[2,8] ten of structure **C**,[9] six of structure **D**,[9] two of structure **E**[3,32] and two of structure **F**[5,6]; one additional compound of structure **F** (phenylazoethenemorpholine) is indicated by Sommer[33] as already known, but we failed to find out any data concerning its preparation and characterization.

2. Chemistry

The syntheses of arylazoenamines of general structures **A**–**D** were carried out as indicated in Scheme 1 by heating the ethanolic solution of relevant carbonyl derivative with the suitable arylhydrazine (or its hydrochloride), concd hydrochloric acid, and 85% phosphoric acid in a molar ratio of 1:2:3:5. Yields were fairly good except when the arylhydrazine is unsubstituted or is substituted with electron-releasing groups. In the last cases a small amount of the corresponding indole was formed and separated by column chromatography.

Starting from 1-methyl-3-piperidone two isomeric compounds, which can be separated by column chromatography, are simultaneously formed (Scheme 2). In all cases, the higher-melting isomer shows the lower R_f in the T.L.C. As previously demonstrated,[9] the low-melting isomer corresponds to the expected 3-arylazo-1-methyl-1,4,5,6-tetrahydropyridine (**C**), while the high-melting one corresponds to 2-arylazo-methylene-1-methylpyrrolidine (**D**). The mechanism of this ring contraction has already been discussed.[9]

The two isomeric compounds could also be obtained starting from the corresponding 2-formyl-1-methylpyrrolidine arylhydrazone, but this procedure is more expensive and does not offer any advantage.

The required octahydro-2*H*-quinolizin-1-one, octahydro-indolizin-8-one, and 1-methyl-3-piperidone were prepared as described in the literature.[34–36] 1-Benzyl-3-piperidone is commercially available.

Compounds of structure **E** were obtained by coupling aryldiazonium salts with 2-methylene-1,3,3-trimethylindoline as indicated by König[4] (Scheme 3).

Finally, compounds of structures **F** and **G** were prepared by condensing glyoxal monoarylhydrazone with the suitable secondary cyclic amine or piperazine (all commercially available) as indicated by Severin et al.[5,6] (Scheme 3).

3. Results and discussion

3.1. Biological activity—general considerations

Title compounds were evaluated for antiviral activity against viruses representative of two of the three genera of Flaviviridae family, that is, Flaviviruses (yellow fever virus, YFV) and Pestiviruses (bovine viral diarrhoea virus, BVDV), as Hepaciviruses can

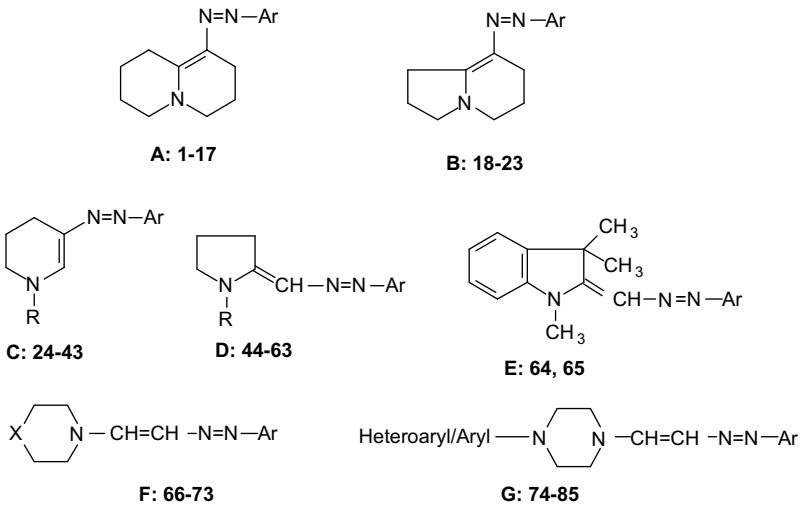

Figure 2. Structures of the investigated compounds.

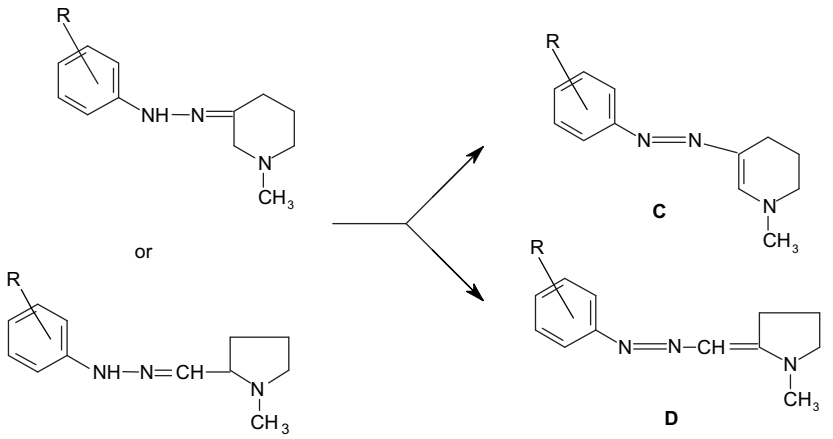

Scheme 2.

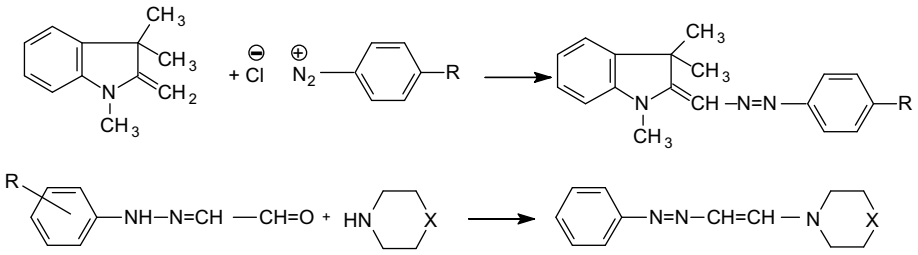

Scheme 3.

hardly be used in routine cell-based assays. Compounds were also tested against representatives of other virus families. Among ssRNA$^+$ were a retrovirus (human immunodeficiency virus type 1, HIV-1) and two Picornaviruses (coxsackie virus type B2, CVB-2 and poliovirus type-1, Sabin strain, Sb-1); among ssRNA$^-$ were a Paramixoviridae (respiratory syncytial virus, RSV) and a Rhabdoviridae (vesicular stomatitis virus, VSV) representative. Among double-stranded RNA (dsRNA) viruses was a Reoviridae representative (Reo-1). Two representatives of DNA virus families were also included: herpes symplex type-1, HSV-1 (Herpesviridae), and vaccinia virus, VV (Poxviridae).

NM-108 (2′-β-methylguanosine), 6-azauridine, AZT (3′-azidothymidine), and ACG (acyclo-guanosine) were used as reference inhibitors of ssRNA$^+$, ssRNA$^-$, HIV-1, and DNA viruses, respectively.

Interestingly, 80 over 85 tested compounds exhibited antiviral activity against one or more viruses: in particular, 27 compounds exhibited a selective activity against a single virus, while 33, 15, 4, and 1 were, respectively, active against two, three, four, and five viruses. None of the test compounds inhibited the multiplication of HIV-1, VSV, and VV, and only three compounds exhibited a modest activity against Reo-1. Similarly, only four compounds displayed moderate activity against HSV-1, but it must be noted that, because of shortage of products, only 50 over 85 compounds were tested against it. In both cases, the observed activity was secondary to the activity on other viruses.

On the other hand, an increasing number of compounds exhibited antiviral activity, sometimes of very high level, against, in the order, Sb-1 (12), YFV (16), BVDV (28), RSV (34), and CVB-2 (62) (Table 1). Twenty-eight of the 62 active compounds inhibited the multiplication of CVB-2 more strongly than the reference compound NM-108 (EC_{50} = 20 μM). Concerning BVDV and RSV, only a few compounds exhibited a EC_{50} value comparable with that of the respective reference drug, NM-108 (EC_{50} = 1.7 μM) and 6-azauridine (EC_{50} = 1.2 μM).

On the whole, 35 compounds have shown an $EC_{50} \leqslant 10$ μM against at least one virus, 28 had EC_{50} between 11 and 30 μM, and only 17 had a EC_{50} in the range 31–100 μM; thus, the arylazoenamine molecular pattern is, indeed, an interesting novel pharmacophore for antiviral agents against ssRNA viruses.

Cytotoxicity and antiviral activities of test and reference compounds are reported in Tables 2–5.

3.2. Cytotoxicity on host cells

Test compounds showed different degrees of cytotoxicity against the confluent cell monolayers (in stationary growth) used to support the multiplication of the different viruses.

The most susceptible to toxicity were the exponentially growing lymphoblastoid human cells (MT-4) used to grow HIV-1, while the non-human host cell lines exhibited a progressively reduced sensitivity in the order MDBK > BHK > Vero-76. Indeed, only 25.9% of compounds showed no toxicity ($CC_{50} \geqslant 100$ μM) against MT-4 versus 47.1% on Vero-76 cells; on the contrary 45.9% of compounds exhibited a $CC_{50} \leqslant 30$ μM for MT-4 compared with 10.6–11.8% in the case of BHK and Vero-76 cells, respectively. CC_{50} so low as 2 μM were found for MT-4 cells, while the lowest CC_{50} values for BHK and Vero-76 were, respectively, 10 and 11 μM.

Cytotoxicity is clearly influenced by the nature of both the amino heads and the arylazo moieties; however, the former seem to be more important than the latter. Considering together the four cell lines, it is observed that the azoethene derivatives of structure **F** and **G** are the most toxic, exhibiting for about 54% a $CC_{50} \leqslant 30$ μM, while the tetrahydropyridines of structure **C** are the least toxic, with only 2.5% of compounds with $CC_{50} \leqslant 30$ μM. Viceversa, ~61% of compounds of the last type showed no toxicity ($CC_{50} \geqslant 100$ μM), while only 15% of compounds **F** and **G** have a CC_{50} in this range. The remaining types of compounds (**A**, **B**, **D**,

Table 1
Number of active compounds on susceptible viruses and range of their EC_{50}

Virus	No. of active over 85 tested compounds[a]	No. of active compounds (range of EC_{50} μM)				
Sb-1[b]	12		2(8)	6(12–27)	1(45)	3(53–60)
YFV[b]	16		4(7–10)	4(12–23)	3(36–48)	5(65–100)
BVDV[b]	28	5(0.8–5.5)	4(6–10)	11(11–21)	2(40, 46)	6(60–100)
RSV[c]	34	6(0.9–5)	6(6–9)	15(11–30)	1(40)	6(60–100)
CVB–2[b]	62	10(0.9–5)	10(6–10)	18(12–30)	13(32–50)	11(51–100)

[a] Compounds with EC_{50} > 100 μM or higher than CC_{50} are considered inactive.
[b] Single-stranded, positive RNA virus.
[c] Single-stranded, negative RNA virus.

and **E**) stay in the middle between the above extremes, with only small differences among them.

The high cytotoxicity observed for a few compounds, particularly against MT-4 cells (i.e., **7**, **12**, **55**, **69**, with CC_{50} = 2–4 μM), while lowering their interest as antivirals, may warrant deeper investigations to obtain novel antiproliferative agents.

3.3. Structure–activity relationships

Also the antiviral activity, as already seen for cytotoxicity, is influenced by the nature of the amino head and the arylazo moiety; while the former seems to mainly address the activity versus the different types of viruses, the latter principally regulate the intensity of the antiviral action. However, in some cases the definition of the real role of each structural feature may result very difficult and even puzzling. Indeed, the shift of a substituent from a position to another of the aromatic moiety may produce a qualitative more than a quantitative variation of activity. Moreover, not all the possible combinations of the basic heads and aromatic moieties could be explored.

Among the five compounds completely devoid of antiviral activity, the lack of activity can be related either to the nature of the basic head (indoline: **64**, **65**), or to the aromatic moiety (3,5-bis-trifluoromethylphenyl: **36**, **55**; pentafluorophenyl: **41**), since the corresponding aromatic moieties of the former and the basic heads of the latter are commonly present in very active compounds.

Despite these shortcomings, some general rules can be drawn.

The arylazohexahydroquinolizines **A** and the arylazoethenamines **F** definitely appear as the most suitable structures for activity against CVB-2; indeed, only one compound (**16**) of the first type and no one of the second failed to inhibit its multiplication.

Also most of the structurally related arylazohexahydroindolizines **B** and arylazoethenepiperazines **G** are active against CVB-2, though acting also against Sb-1 and RSV, respectively. About a half of compounds active against RSV is found in groups **F** and **G**; the remaining being evenly distributed among the others.

Interestingly, no one of compounds of **F** and **G** groups was active against BVDV.

The arylazotetrahydropyridines **C** and the arylazomethylenepyrrolidines **D** share in almost equal measure the activity against CVB-2 and BVDV or on both types of viruses. It is worth noting that the exchange of the methyl group with a benzyl abolishes the activity against BVDV, leaving or enhancing that against CVB-2.

Sole activity on YFV is never found in any tested compound, but in association with activity on CVB-2 and/or BVDV is most commonly found among arylazoenamines **F** and arylazoethenepiperazines **G**. Activity against YFV is shown by only 1 over 17 compounds of group **A**, but by none of group **B**.

Selective activity on Sb-1 is shown by a single compound of group **C**, while activity on Sb-1 associated with activity on CVB-2 and BVDV is exhibited by several compounds of the same and other groups, especially by hexahydroindolizines **B**.

Compounds endowed with the highest activity against a given virus may also be selective for it (**26**: EC_{50} = 8 μM for Sb-1; **32**: EC_{50} = 0.8 μM for BVDV; **84**: EC_{50} = 0.9 μM for RSV), or may exhibit simultaneously good activity on one or two other viruses, as compound **75** (EC_{50} = 0.9 μM for CVB-2) and **47** (EC_{50} = 7 μM for YFV) that inhibit also, respectively, RSV and BVDV and CVB-2 with EC_{50} in the range 5–16 μM.

Generally, compounds acting on three or more viruses display only a moderate or even a modest degree of activity. Interesting exceptions are represented by compounds **28**, **47**, **76**, **83,** and, particularly, **81**, that exhibited a EC_{50} = 7 μM against CVB-2, YFV and RSV. Most of the nineteen large spectrum compounds belong (13/19) to groups **C** and **D**; the remaining are found in groups **G** (3/19), **A** (2/19), and **B** (1/19).

3-(4-Chlorophenylazo)-1-methyltetrahydropyridine (**28**) is active on Sb-1, CVB-2, RSV and Reo virus, with EC_{50} = 8, 5, 20 and 32 μM, respectively. The shift of chlorine from *para* to *ortho* position (**26**) produces the loss of the activity on CVB-2, RSV and Reo viruses, leaving unchanged that on Sb-1; however when the chlorine is placed on *meta* position (**27**) the activity on CVB-2 and RSV is maintained (though reduced), but that on Sb-1 and Reo is lost, while appears a good activity on BVDV. The activity on Sb-1 is lost also when the 4-chlorophenylazo substituent of compound **28** is attached on the methylenepyrrolidine moiety (**46**) that is isomeric to the tetrahydropyridine ring of **28**. Curiously, compound **46** exhibits the same spectrum of activity (CVB-2, RSV, and BVDV) of the meta chloro derivative **27**. Differently from what is observed for the isomeric 4-chlorophenylazo derivatives **28** and **46**, the isomeric 3-nitrophenylazo compounds **32** and **50** maintain a high and selective activity against BVDV.

The varied activities shown by the four isomeric compounds **26**, **27**, **28**, and **46** demonstrate the intriguing complexity of the structure–activity relationships for this kind of compounds. Therefore, in an attempt to reach a better understanding of the structural requirements for antiviral activity on the 85 arylazoenamines **A**–**G**, a ligand-based computational approach was employed in order to derive a highly predictive pharmacophore model for the most frequently affected viruses CVB-2, RSV, and BVDV. Results of this study are discussed in the next section.

Despite the high antiviral activity of many compounds, the corresponding selectivity indexes (SI) are most commonly below 10, due to the high toxicity on the host cells often observed. Nevertheless, 17 compounds exhibited a selectivity index in the range from >10 to >125, for at least one of the viruses CVB-2, BVDV, RSV, and Sb-1. The reference compound NM-108 exhibits a SI >5 and >58.8 for CVB-2 and BVDV viruses, respectively.

Thus, taking into account the EC_{50} and SI values, the best compounds can be arranged in the following order of decreasing potency and selectivity; for CVB-2: **75** > **66** ⩾ **53** ⩾ **28**; for BVDV: **32** > **22** > **42** = **50** > **16**; for RSV: **84** > **23,** and for Sb-1: **26** ⩾ **28**. In these sequences even the least potent compounds compare well with the reference compounds. It must be observed, however, that in view of a therapeutical application the cytotoxicity on human

Table 2
Cytotoxicity against MT-4, MDBK, BHK and Vero-76 cell lines and BVDV, YFV, CVB-2, RSV, and Sb-1 inhibitory activity of arylazoenamines of structures **A** and **B**

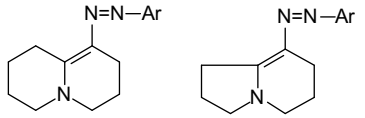

A: 1-17 **B: 18-23**

Compound	Aryl=	MT-4 CC_{50}[a] (μM)	MDBK CC_{50}[b] (μM)	BVDV EC_{50}[c] (μM)	BHK CC_{50}[d] (μM)	YFV EC_{50}[e] (μM)	Vero-76 CC_{50}[f] (μM)	CVB-2 EC_{50}[g] (μM)	RSV EC_{50}[h] (μM)	Sb-1 EC_{50}[i] (μM)
1	4-F-Ph[l]	94	56	>56	>100	100	>100	27	>100	>100
2	2-Cl-Ph	78	>100	>100	93	>93	>100	32	60	>100
3	3-Cl-Ph	16	20	>20	46	>46	60	22	18	>60
4	4-Cl-Ph	42	60	>60	69	>69	80	19	25	>80
5	3-Br-Ph	9	10	>10	49	>49	>100	18	>100	>100
6	4-Br-Ph	27	59	>59	62	⩾62	92	10	>92	>92
7	3-CF_3-Ph	4	8	>8	40	>40	>100	21	>100	>100
8	3-NO_2-Ph	37	>100	>100	87	>87	90	71	>90	20
9	4-NO_2-Ph	91	>100	86	>100	⩾100	100	26	>100	>100
10	3,4-DiCl-Ph	35	30	>30	54	>54	>100	38	>100	>100
11	3,5-DiCF_3-Ph	34	31	>31	19	>19	100	41	>100	>100
12	3-CF_3-4-F-Ph	3	>100	>100	60	>60	>100	45	>100	>100
13	3-CF_3-4-Cl-Ph	19	35	>35	41	>41	>100	64	>100	>100
14	3-CF_3-4-Br-Ph[m]	34	>100	61	>100	80	100	42	>100	25
15	3-NO_2-4-Cl-Ph	33	18	>18	10	>10	100	51	75	>100
16	1-Naphthyl	12	>100	6	20	>20	90	>90	>90	>90
17	7-Chloro-1-quinolyl	15	40	5	48	>48	85	51	>85	>85
18	4-Cl-Ph	>100	30	>30	34	>34	75	10	>75	20
19	3-NO_2-Ph	>100	68	>68	95	>95	>100	54	>100	60
20	3,4-DiCl-Ph	26	67	>67	61	>61	>100	30	>100	45
21	3-CF_3-4-Cl-Ph[n]	30	21	>21	51	>51	100	9	>100	12
22	1-Naphthyl	18	91	3.5	51	>51	90	44	>90	>90
23	1-Phthalazyl	52	>100	>100	>100	>100	>100	>100	7	>100
NM-108 (2′-β-methylguanosine)		>100	>100	1.7	90	1	>100	20	>100	>100
6-Azauridine		2	>100	>100	>100	26	20	>20	1.2	>20

[a] Compound concentration (μM) required to reduce the viability of mock-infected MT-4 ($CD4^+$ human T cells containing an integrated HTLV-1 genome) cells by 50%, as determined by the MTT method.
[b] Compound concentration (μM) required to reduce the viability of mock-infected MDBK (bovine normal kidney) cells by 50%, as determined by the MTT method.
[c] Compound concentration (μM) required to achieve 50% protection of MDBK cells from BVDV (bovine viral diarrhoea virus) induced cytopathogenicity, as determined by the MTT method.
[d] Compound concentration (μM) required to reduce the viability of mock-infected BHK (hamster normal kidney fibroblast) monolayers by 50%, as determined by the MTT method.
[e] Compound concentration (μM) required to achieve 50% protection of BHK cells (kidney fibroblast) from YFV (yellow fever virus) induced cytopathogenicity, as determined by the MTT method.
[f] Compound concentration (μM) required to reduce the viability of mock-infected VERO-76 (monkey normal kidney) monolayers by 50%.
[g] Compound concentration (μM) required to reduce the plaque number of CVB 2 (coxsackie virus B2) by 50% in VERO-76 monolayers.
[h] Compound concentration (μM) required to reduce the plaque number of RSV (respiratory syncitial virus) by 50% in VERO-76 monolayers.
[i] Compound concentration (μM) required to reduce the plaque number of Sb-1 (poliovirus type-1, Sabin strain) by 50% in VERO-76 monolayers.
[l] Active also on Reo-1 virus (EC_{50} = 34 μM).
[m] Active also on HSV-1 virus (EC_{50} = 25 μM).
[n] Active also on HSV-1 virus (EC_{50} = 33 μM).

Table 3
Cytotoxicity against MT-4, MDBK, BHK, and Vero-76 cell lines and BVDV, YFV, CVB-2, RSV, and Sb-1 inhibitory activity of arylazoenamines of structure **C**

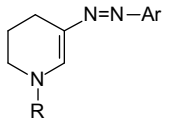

C: 24-43

Compound	Aryl=	MT-4 CC_{50}[a] (μM)	MDBK CC_{50}[b] (μM)	BVDV EC_{50}[c] (μM)	BHK CC_{50}[d] (μM)	YFV EC_{50}[e] (μM)	Vero-76 CC_{50}[f] (μM)	CVB-2 EC_{50}[g] (μM)	RSV EC_{50}[h] (μM)	Sb-1 EC_{50}[i] (μM)
R = CH_3										
24	Phenyl	>100	>100	>100	>100	>100	⩾100	>100	75	>100
25	4-F-Ph	⩾100	48	>48	90	>90	77	53	30	>77
26	2-Cl-Ph	>100	>100	100	>100	>100	>100	>100	>100	8
27	3-Cl-Ph	>100	87	12	85	>85	75	34	40	>75
28	4-Cl-Ph[l]	>100	58	>58	>100	>100	90	5	20	8
29	3-Br-Ph	>100	>100	19	>100	71	>100	27	18	>100
30	4-Br-Ph[m]	83	>100	60	>100	100	100	>100	18	>100
31	3-CF_3-Ph	>100	>100	90	>100	>100	>100	>100	>100	>100
32	3-NO_2-Ph	>100	>100	0.8	95	>95	>100	>100	>100	>100
33	4-NO_2-Ph	>100	62	11	>100	>100	>100	>100	>100	>100
34	4-CH_3-Ph	>100	>100	>100	>100	>100	71	>71	>71	25
35	3,4-DiCl-Ph	43	73	7	38	>38	>100	14	>100	>100
36	3,5-DiCF_3-Ph	>100	64	>64	82	>82	>100	>100	>100	>100
37	3-CF_3-4-F-Ph	>100	>100	>100	80	>80	70	35	>70	>70
38	3-CF_3-4-Cl-Ph	62	28	>28	44	>44	90	34	>90	>90
39	3-CF_3-4-Br-Ph	50	>100	40	>100	>100	80	40	>80	>80
40	3-NO_2-4-Cl-Ph	71	61	>61	>100	>100	>100	>100	>100	>100
41	PentaF-Ph	>100	>100	>100	>100	>100	>100	>100	100	>100
42	1-Naphthyl	>100	>100	5	>100	>100	⩾100	76	>100	>100
R = CH_2-C_6H_5										
43	3-CF_3-4-Cl-Ph	43	28	⩾28	32	22	48	4	>48	>48
NM-108 (2′-β-methylguanosine)		>100	>100	1.7	90	1	>100	20	>100	>100
6-azauridine		2	>100	>100	>100	26	20	>20	1.2	>20

For the meaning of [a–i]: see Table 2.
[l]Active also on Reo-1 virus (EC_{50} = 32 μM). [m]Active also on Reo-1 virus (EC_{50} = 76 μM).

Table 4
Cytotoxicity against MT-4, MDBK, BHK, and Vero-76 cell lines and BVDV, YFV, CVB-2, RSV, and Sb-1 inhibitory activity of arylazoenamines of structures **D** and **E**

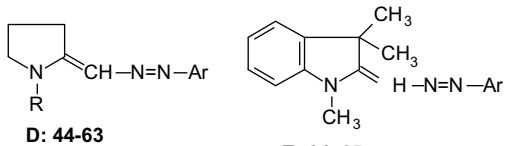

D: 44-63 **E: 64, 65**

Compound	Aryl=	MT-4 CC_{50}[a] (μM)	MDBK CC_{50}[b] (μM)	BVDV EC_{50}[c] (μM)	BHK CC_{50}[d] (μM)	YFV EC_{50}[e] (μM)	Vero-76 CC_{50}[f] (μM)	CVB-2 EC_{50}[g] (μM)	RSV EC_{50}[h] (μM)	Sb-1 EC_{50}[i] (μM)
R=CH_3										
44	Phenyl	>100	>100	10	>100	>100	82	19	20	>82
45	4-F-Ph	100	59	18	80	36	75	>75	12	>75
46	4-Cl-Ph	>100	85	21	55	⩾55	92	24	20	>92
47	3-Br-Ph	55	52	9	41	7	80	16	>80	>80
48	4-Br-Ph	23	>100	11	>100	>100	100	36	20	>100
49	3-CF_3-Ph	49	90	21	50	>50	>100	>100	>100	>100
50	3-NO_2-Ph	25	>100	5.5	>100	>100	>100	>100	>100	>100
51	4-NO_2-Ph[l]	>100	>100	19	>100	65	>100	79	75	>100
52	4-CH_3-Ph	>100	>100	20	>100	>100	>100	60	>100	>100
53	4-CH_3O-Ph	>100	67	18	77	>77	100	5	>100	>100
54	3,4-diCl-Ph[m]	39	90	16	23	>23	100	>100	>100	53
55	3,5-diCF_3-Ph	2	36	>36	48	>48	93	>93	>93	>93
56	3-CF_3-4-F-Ph[n]	11	>100	100	41	>41	>100	71	>100	>100
57	3-CF_3-4-Br-Ph	24	>100	46	>100	>100	⩾100	100	>100	60
58	PentaF-Ph	8	>100	>100	>100	>100	>100	>100	75	>100
R=CH_2-C_6H_5										
59	Phenyl	22	74	>74	31	>31	87	16	30	>87
60	4-Cl-Ph	17	18	>18	20	>20	70	23	>70	>70
61	4-CH_3-Ph	10	22	>22	25	>25	50	8	>50	>50
62	3,4-diCl-Ph[o]	19	79	>79	50	>50	55	21	>55	>55
63	3-CF_3-4-Cl-Ph	20	14	>14	22	>22	80	30	>80	>80
64	Phenyl[p]	30	20	>20	47	>47	73	>73	>73	>73
65	4-Cl-Ph	55	72	>72	21	>21	>100	>100	>100	>100
NM-108 (2′-β-methylguanosine)		>100	>100	1.7	90	1	>100	20	>100	>100
6-Azauridine		2	>100	>100	>100	26	20	>20	1.2	>20

For the meaning of[a–i]: see Table 2; [l]mixture (2:1) with **C** isomer as seen from NMR spectrum; [m]active also on HSV-1 virus (EC_{50} = 40 μM); [n]active also on HSV-1 virus (EC_{50} = 60 μM); [o]mixture (3:1) with **C** isomer as seen from NMR spectrum; [p]as perchlorate.

Table 5
Cytotoxicity against MT-4, MDBK, BHK, and Vero-76 cell lines and BVDV, YFV, CVB-2, RSV, and Sb-1 inhibitory activity of arylazoenamines of structures **F** and **G**

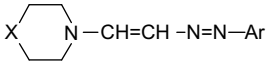

F: 66-73

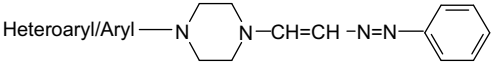

G: 74-85

Compound	X=	Ar=	MT-4 CC_{50}[a] (μM)	MDBK CC_{50}[b] (μM)	BVDV EC_{50}[c] (μM)	BHK CC_{50}[d] (μM)	YFV EC_{50}[e] (μM)	Vero-76 CC_{50}[f] (μM)	CVB-2 EC_{50}[g] (μM)	RSV EC_{50}[h] (μM)	Sb-1 EC_{50}[i] (μM)
66	/	Phenyl	8	63	>63	82	>82	70	4	30	>70
67	/	4-Cl-Ph	61	30	>30	>100	46	22	4	>22	>22
68	/	4-EtO-CO-Ph	26	100	>100	>100	>100	>100	50	>100	>100
69	CH_2	Ph	2	7	>7	67	23	15	7	>15	>15
70	CH_2	4-EtO-CO-Ph	33	>100	>100	>100	>100	>100	35	>100	27
71	O	Ph	7	28	>28	>100	>100	30	7	15	>30
72	S	Ph	19	14	>14	>100	>100	30	6	>30	>30
73	EtO-CON	Ph	17	13	>13	>100	>100	30	12	4	>30
74	2-Pyridinyl		19	⩾100	>100	75	>75	22	6	7	>22
75	2-Pyrimidinyl		17	10	>10	>100	>100	55	0.9	5	>55
76	Phenyl		15	5	>5	60	42	50	5	11	>50
77	2-F-Ph		32	10	>10	62	>62	34	6	6	>34
78	4-F-Ph		17	13	>13	50	20	35	5	9	>35
79	2-Cl-Ph		16	13	>13	69	>69	14	5	5	>14
80	3-Cl-Ph		19	7	>7	47	10	11	>11	5	>11
81	4-Cl-Ph		21	7.5	>7.5	29	7.5	45	7	7	>45
82	3-CF_3-Ph		30	9	>9	43	9	11	>11	4	>11
83	4-NO_2-Ph		41	20	>20	48	12	45	14	13	>45
84	4-CH_3CO-Ph		21	8	>8	49	>49	11	>11	0.9	>11
85	4-CH_3O-Ph		29	19	>19	46	>46	38	5	6	>38
NM-108 (2′-β-methylguanosine)			>100	>100	1.7	90	1	>100	20	>100	>100
6-Azauridine			2	>100	>100	>100	26	20	>20	1.2	>20

For the meaning of[a–i]: see Table 2.

cells is more significant than that on host cells, and therefore, among the foregoing sequences, compounds **53**, **28**, **32**, and **42** appear of high interest being devoid of toxicity on the human MT-4 cells (CC_{50} > 100 μM).

3.4. Molecular modeling

3.4.1. Pharmacophore models generation

It is a widely accepted concept that three-dimensional (3D) pharmacophore modeling is a well-behaved approach to quantitatively explore the common chemical characteristics among a considerable number of different structures. Indeed, a computed pharmacophore model can, in principle, be as good as the information data input. Nevertheless, to achieve such a quality, at least three must obey rules should be respected in a three-dimensional quantitative structure–activity relationship (3D-QSAR) generation using *CATALYST*: (i) the training set must be constituted by a wide population (at least 16 items) of structurally diverse representative covering at least four orders of magnitude of activity, (ii) the most active compound should inevitably be included in the training set, and (iii) all biological data must be obtained by homogeneous procedures.

In our case, three training sets (TrS)—consisting of 18, 43, and 21 compounds for BVDV, CVB-2, and RSV, respectively—were prepared by considering structural diversities and by the widest coverage of in vitro activity range possible (see Table 6). The molecules in each TrS were selected according to the following criteria: (i) each TrS for each virus should contain structures from each class of active compounds and (ii) each TrS should cover the molecular bioactivities (EC_{50}) as widely as possible. Should there be only one compound with maximum or minimum order of bioactivity in a class, this compound had to be assigned to the training set. Compounds **51** and **62**, although active against BVDV and/or CVB-2, were not included in the corresponding training sets as they were experimentally tested as a mixture of isomers.

A set of 10 hypotheses was automatically generated for each of the three BVDV_TrS, CVB-2_TrS, and RSV_TrS training sets using the *HypoGen* module in *CATALYST*. Hydrophobic aromatic (HAr) sites, hydrogen bond acceptor (HBA), hydrogen bond donor (HBD), positive ionizable (PI), and ring aromatic (RAr) moieties were selected as the functional features to describe the antiviral activity of the compounds. The best predictive hypothesis (Hypo1) for each training set obtained from *HypoGen* has three features for BVDV, and two features for CVB-2 and RSV. In detail, Hypo1_BVDV is characterized by two hydrogen bond donors and one hydrophobic aromatic, while both Hypo1_CVB-2 and Hypo1_RSV have one hydrogen bond donor and one aromatic ring (see Fig. 3). These three hypotheses were also all characterized by the highest cost differences, the lowest root-mean-square (RMSD) deviations, and the highest correlation coefficients (see below).

In harmony with the predicted activities, the three most active compounds in the three TrSs (i.e., compounds **32** in BVDV_TrS, **75** in CVB-2_TrS, and **84** in RSV_TrS in Table 6) can be nicely mapped onto the corresponding Hypo1 models by the best fit values, as can be appreciated from Figure 4. As we can see from this figure, compound **32** fits very well all features of the pharmacophore model Hypo1_BVDV. In fact, the first HBA is located on the nitro group, the phenyl moiety overlaps with the HAr feature, and the second HBA is mapped by the aza group. Noticeably, although the other two hypotheses possess the same chemical features, the different relative orientations and distances of these groups in the two cases impose different mapping modes. Thus, in the case of compound **75**, it is the aromatic ring bound to the aza group that overlaps neatly over the RAr site, while one of the two nitrogen of the pyrimidine substituent serves as an HBA in Hypo1_CVB-2. On the other hand, the aromatic moiety of the acetylphenyl substituent of **84** disposes over the RAr feature of Hypo1_RSV, whereas one nitrogen atom of the aza group again maps the remaining HBD feature.

As expected, for the majority of the less active compounds we found that they do not map adequately or eventually miss some of the relevant hypothesis features; for some of these molecules, their lack of affinity could be primarily ascribed to their inability to achieve an energetically favorable conformation required by the pharmacophore and shared by the active compounds.

Taken together, all these evidences concur to indicate that each Hypo1 model provides reasonable pharmacophoric characteristics of the three virus inhibitors for the components of their corresponding activities.

3.4.2. Cost analysis

When generating an hypothesis, *CATALYST* performs a *fixed cost* calculation, which represents the simplest model that fits all data perfectly, and a *null cost* calculation, which presumes that there is no relationship in the data set, and that the experimental activities are normally distributed about their mean. Accordingly, a generated pharmacophore hypothesis with a score that is substantially lower than that of the corresponding null hypothesis is likely to be statistically significant. Two further criteria should be satisfied in assessing the validity of a given hypothesis: (a) the cost of the hypothesis should be close to the fixed cost and (b) the *configurational cost*, that is the magnitude of the hypothesis space for a given TrS of compounds, should be less than 17. If this last cost exceeds 17, there are more degrees of freedom in the TrS that the *CATALYST* algorithm can properly handle and, consequently, the corresponding pharmacophore is likely to be poorly meaningful.

The quality of the three statistically most significant hypotheses out of the ten generated by *HypoGen* for each TrSs (Hypo1_BVDV, Hypo1_CVB-2, and Hypo1_RSV, respectively) was evaluated by considering the relevant cost functions (see Table 7).

Detailedly, for BVDV the cost range between Hypo1_BVDV and the fixed cost is 8.59, while that between the null hypothesis and Hypo1_BVDV is 77.69 (see Table 7, first row). According to these scores, criterion (a) is satisfied as the total cost of Hypo1_BVDV is much closer to the fixed cost than to the null cost. Furthermore, a high correlation coefficient (ρ) of 0.98, a RMSD value of 0.50, and a configurational cost of 12.78 (criterion (b)) allow us to conclude that Hypo1_BVDV is a reliable pharmacophore model with high predictivity for our compounds. Treating the 43 test compounds active against CVB-2 with *HypoGen* yielded the corresponding best hypothesis Hypo1_CVB-2 (see Table 7, second row), characterized by a total cost of 107.92. The total fixed cost for this run was 89.62 and the cost of the null hypothesis was 173.57. Thus, the large difference between the null and total hypothesis costs (65.65) and the closeness of the hypothesis cost to the fixed total cost (18.30), coupled with a low configurational cost (13.56), a good RMSD (0.94), and a high ρ value (0.97), all speak in favor of the statistical significance of the top-ranked hypothesis. Finally, also for Hypo1_RSV the ample difference between the null and total hypothesis cost (79.85), the high correlation coefficient (0.95), and the excellent RMSD value (0.38) (see Table 7, last row) indicates a reliable predictivity of the corresponding 3D-QSAR pharmacophore and confirm that it is not a chance correlation.

3.4.3. Validation of the pharmacophore models

To cross-validate the observed correlations, we prepared three test sets (TsS) of further 9, 17, and 12 compounds for BVDV, CVB-2, and RSV, respectively. Interestingly, good correlation coefficients (0.97, 0.95, and 0.96) were observed when a regression analysis was performed by mapping each test set onto the features of the corresponding best pharmacophore hypothesis. The predicted and the experimental EC_{50} values for the three TsSs along with

Table 6
Estimated and experimentally determined activity values of the training set compounds for BVDV, CVB-2, and RSV

BVDV				CVB-2				RSV			
Training set compounds	$EC_{50,exp.}$ (μM)	$EC_{50,est.}$ (μM)	Error[a]	Training set compounds	$EC_{50,exp.}$ (μM)	$EC_{50,est.}$ (μM)	Error[a]	Training set compounds	$EC_{50,exp.}$ (μM)	$EC_{50,est.}$ (μM)	Error[a]
32	0.8	0.9	1.1	**75**	0.9	1.6	1.8	**84**	0.9	1.1	1.2
22	3.5	7.9	2.3	**43**	4	5.8	1.5	**73**	4	7.2	1.8
42	5	3	−1.7	**66**	4	3.1	−1.3	**82**	4	4.1	1.0
17	5	7.8	1.6	**28**	5	7	1.4	**75**	5	4.5	−1.1
50	5.5	4.6	−0.8	**53**	5	2.2	−2.3	**79**	5	5	1.0
47	9	15	1.7	**76**	5	5.8	1.2	**77**	6	5	−1.2
33	11	13	1.2	**79**	5	6	1.2	**23**	7	10	1.4
27	12	19	1.6	**85**	5	5.3	1.1	**76**	11	9.6	−1.1
45	18	12	−1.5	**72**	6	5.9	−1.0	**45**	12	15	1.3
53	18	19	1.1	**77**	6	6	1.0	**83**	13	10	−1.3
52	20	26	1.3	**69**	7	5	−1.4	**71**	15	18.9	1.3
49	21	16	−1.3	**71**	7	10	1.4	**30**	18	19	1.1
39	40	41	1.0	**61**	8	12	1.5	**44**	20	34	1.7
30	60	55	−1.1	**21**	9	15	1.7	**48**	20	32	1.6
14	61	58	−1.1	**18**	10	9	−1.1	**4**	25	34	1.4
9	86	93	1.1	**6**	10	16	1.6	**59**	30	29	−1.0
31	90	94	1.0	**73**	12	10	−1.2	**66**	30	34	1.1
56	100	96	−1.0	**35**	14	13	−1.1	**27**	40	33	−1.2
				83	14	6.9	−2.0	**15**	75	68	−1.1
				59	16	11	−1.5	**58**	75	65	−1.1
				47	16	20	1.3	**41**	100	93	−1.1
				4	19	23	1.2				
				60	23	13	−1.8				
				46	24	28	1.2				
				29	27	26	−1.0				
				1	27	28	1.0				
				2	32	35	1.1				
				38	34	31	−1.1				
				37	35	31	−0.9				
				48	36	30	−1.2				
				14	42	38	−1.1				
				22	44	42	−1.0				
				12	45	44	−1.0				
				68	50	58	1.2				
				17	51	51	1.0				
				15	51	56	1.1				
				25	53	48	−1.1				
				19	54	55	1.0				
				52	60	67	1.1				
				13	64	70	1.1				
				8	71	81	1.1				
				42	76	66	−1.2				
				57	100	108	1.1				

[a] Value in the error column represent the ratio of the estimated activity to measured activity, or its negative inverse if the ratio is less than one.

the respective errors are shown in Table 8. The actual activity values are within the limits of uncertainty (i.e., 2.0), thus confirming the validity of the original 3D pharmacophores.

A final evaluation of the statistical relevance of the 3D pharmacophore models, the Fisher method was applied using the *CatScramble* program available in the *CATALYST* suite of programs. According to the validation procedure, the experimental activity of the compounds in each training test was scrambled randomly, and the resulting new training set was used for a new *HypoGen* run. The parameters adopted in running these calculations were the same employed in the initial *HypoGen* calculations and, since a 98% confidence level was selected, 49 random hypotheses were generated. The resulting data clearly indicate that all values generated after randomization produced hypotheses with no predictive values similar or close to the corresponding Hypo1s. Indeed, none of the outcome hypotheses has lower cost score, better correlation or smaller root-mean-square deviation than the initial one. Table 9 lists the first 10 lowest total score values of the resulting 49 hypotheses for BVDV, CVB-2, and RSV, respectively. In conclusion, there is a 98% chance for the best hypothesis to represent a true correlation in the training set activity data for each antiviral class of compounds.

4. Conclusions

Several sets of arylazoenamines (**A**–**G**, for a total of 85 compounds), characterized by different types of aryl and basic moieties, have been synthesized and assayed for antiviral activity against a panel of ten RNA and DNA viruses. Eighty over 85 compounds exhibited selective or large spectrum antiviral activity; in particular, 12 were active on Sb-1, 16 on YFV, 28 on BVDV, 34 on RSV, and 62 on CVB-2. Two viruses (Reo-1 and HSV-1) were susceptible only to very few compounds; the remaining (HIV-1, VSV, and VV) were not affected by any compound.

Thirty-five compounds have shown high activity, with EC_{50} in the range 0.8–10 μM, against at least one virus and other 28 compounds had EC_{50} between 11 and 30 μM, thus indicating that the arylazoenamine molecular pattern is an interesting novel pharmacophore for antiviral agents against ssRNA viruses.

Some interesting correlations between the structure and the type of affected virus were shown. The arylazohexahydroquinolizines **A** and the aryazoethenamines **F** appear as the most suitable structures for activity on CVB-2. The arylazotetrahydropyridines **C** and the arylazomethylenepyrrolidines **D** share in almost equal measure the activity on CVB-2 and BVDV, while the RSV was

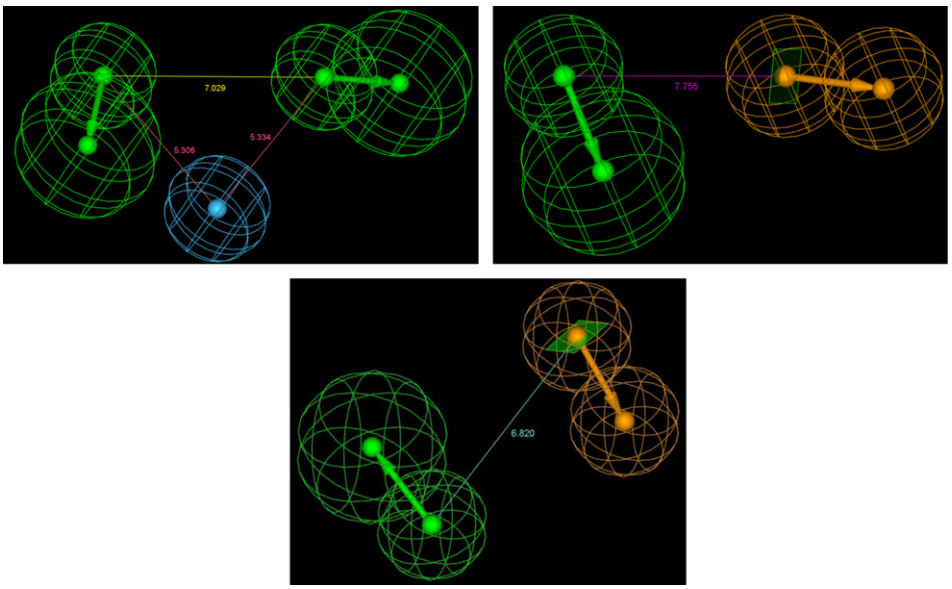

Figure 3. Top scoring *HypoGen* pharmacophore for BVDV (top, left), CVB-2 (top, right), and RSV (bottom, center). Hypothesis features are color-coded as follows: cyan, hydrophobic aromatic (HAr); green, hydrogen bond acceptor (HBA), dark gold, aromatic ring (RAr). The distances (Å) between all features in the corresponding hypotheses are also shown.

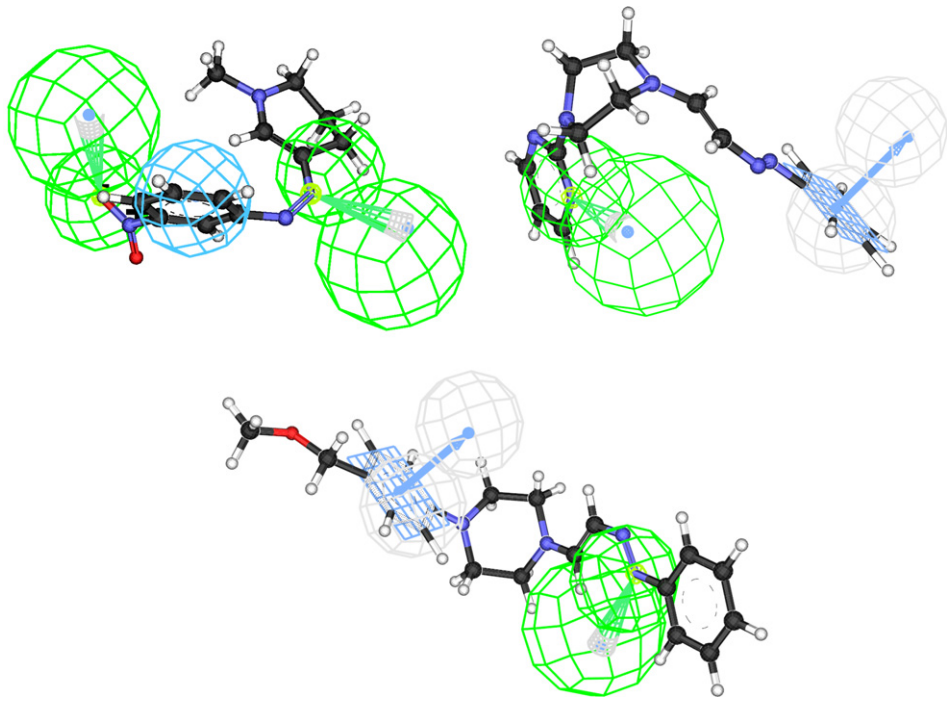

Figure 4. Mapping of the three most active compounds of the training sets onto the corresponding top-ranked 3D pharmacophore models (top, left), compound **32** onto Hypo1_BVDV; (top, right), compound **75** onto Hypo1_CVB-2; (bottom, center) compound **84** onto Hypo1_RSV. Hypothesis features are color-coded as follows: cyan, hydrophobic aromatic (HAr); green, hydrogen bond acceptor (HBA), light blue/gray, aromatic ring (RAr).

Table 7
Results for the best pharmacophore hypotheses (Hypo1) generated by *CATALYST HypoGen* using the training sets for BVDV, CVB-2, and RSV

Hypotheses	Total fixed cost	Total Hypo1 cost	Null cost	Configurational cost	RMSD[a]	ρ	Features
Hypo1_BVDV	93.89	102.48	180.17	12.78	0.50	0.98	HBA, HBA, HAr
Hypo1_CVB-2	89.62	107.92	173.57	13.56	0.42	0.97	HBA, RA
Hypo1_RSV	103.01	121.15	201.00	14.23	0.38	0.95	HBA, RA

All cost units are in bits.
[a] Defined in terms of the deviation of the log(estimated activity), from the log(experimental activity), normalized by the log(uncertainty).

Table 8
Estimated and experimentally determined activity values of the test set compounds for BVDV, CVB-2, and RSV

BVDV				CVB-2				RSV			
Test set compounds	$EC_{50,exp.}$ (μM)	$EC_{50,est}$ (μM)	Error[a]	Test set compounds	$EC_{50,exp.}$ (μM)	$EC_{50,est}$ (μM)	Error[a]	Test set compounds	$EC_{50,exp.}$ (μM)	$EC_{50,est.}$ (μM)	Error[a]
16	6	8	1.3	**67**	4	3.5	−1.1	**80**	5	4.9	−1.0
35	7	9	1.3	**78**	5	6.4	1.3	**85**	6	7	1.2
44	10	19	1.9	**74**	6	5.5	−1.1	**81**	7	8.5	1.2
48	11	13	1.2	**81**	7	6.6	−1.1	**74**	7	6	−1.2
54	16	14	−1.1	**5**	18	18	1.0	**78**	9	12	1.3
29	19	13	−1.5	**44**	19	21	1.1	**3**	18	16	−1.1
46	21	25	1.2	**7**	21	19	−1.1	**29**	18	20	1.1
57	46	40	−1.2	**3**	22	28	1.3	**28**	20	19	−1.1
26	100	94	−1.1	**9**	26	25	−1.0	**46**	20	24	1.2
				20	30	28	−1.1	**25**	30	24	−1.3
				63	30	29	−1.0	**2**	60	51	−1.2
				27	34	38	1.1	**24**	75	64	−1.2
				70	35	28	−1.3				
				10	38	33	−1.2				
				39	40	44	1.1				
				11	41	38	−1.1				
				56	71	62	−1.1				

[a] Values in the error column represent the ratio of the estimated activity to measured activity, or its negative inverse if the ratio is less than one.

Table 9
Output parameters of the 10 lowest cost hypotheses resulting from the statistical evaluation according to the *Cat-Scramble* validation procedure for BVDV, CVB-2, and RSV

BVDV				CVB-2				RSV			
Hypothesis	ρ	RMSD	Total cost	Hypothesis	ρ	RMSD	Total cost	Hypothesis	ρ	RMSD	Total cost
1	0.77	0.75	131.66	1	0.84	0.91	158.04	1	0.74	0.68	155.35
2	0.76	0.78	133.14		0.84	0.93	159.51		0.72	0.75	157.87
3	0.76	0.79	133.75	2	0.81	1.02	181.09	2	0.68	0.84	161.69
4	0.74	0.80	135.22	3	0.79	1.01	183.63	3	0.66	0.90	168.21
5	0.73	0.81	137.29	4	0.78	1.05	184.64	4	0.63	0.96	169.97
6	0.71	0.84	140.01	5	0.75	1.13	190.07	5	0.61	0.99	170.30
7	0.71	0.88	141.56	6	0.75	1.21	192.55	6	0.57	1.05	174.08
8	0.69	0.92	142.81	7	0.73	1.24	193.78	7	0.55	1.08	174.53
9	0.66	1.01	144.35	8	0.73	1.25	194.16	8	0.52	1.14	178.04
10	0.64	1.11	145.22	10	0.72	1.26	198.23	10	0.47	1.21	181.69
Hypo1	0.98	0.50	102.48	Hypo1	0.97	0.42	107.92	Hypo1	0.95	0.38	121.15

mainly affected by arylazoethenepiperazines **G**. Many compounds exhibited a selectivity index (CC_{50} for host cells/EC_{50} for a given virus) in the range from >10 to >125.

Taking into account the EC_{50} and SI values, the best compounds can be arranged in the following order of decreasing potency and selectivity; for CVB-2: **75** > **66** ⩾ **53** ⩾ **28**; for BVDV: **32** > **22** > **42** = **50** > **16**; for RSV: **84** > **23**, and for Sb-1: **26** ⩾ **28**. In these sequences, even the least potent compounds still compare well with the reference drugs NM-108 and 6-azauridine.

Compounds **53**, **28**, **32**, and **42** appear of particular interest being also devoid of toxicity on the human MT-4 cells (CC_{50} > 100 μM).

A ligand-based computational approach was employed to identify molecular structure requirements in the available series of compounds to act as effective viral inhibitors. Three highly predictive pharmacophore models were generated based on 18, 43, and 21 training set compounds for BVDV, CVB-2, and RSV, respectively, which consist of two hydrogen bond donors and one hydrophobic aromatic in the case of BVDV (Hypo1_BVDV), and one hydrogen bond donor and one ring aromatic for the two other viral species (Hypo1_CVB-2 and Hypo1_RSV, respectively). The application of our 3D pharmacophore models to three test sets of different compounds showed that each model is able to accurately predict the activity of the compounds toward the respective virus. Since the target proteins for the antiviral activities of our series of compounds is as yet unknown, our three-dimensional QSAR pharmacophore models should constitute useful tools in the design of second generations of different, more potent inhibitors of these human and veterinary pathogens.

5. Experimental

5.1. General

Chemicals, solvents, and reagents used for syntheses were purchased from Sigma–Aldrich, Fluka, or Lancaster, and were used without any further purification, unless otherwise specified. Not commercially available arylhydrazines, as 4-F-3-CF_3,[37] 4-Cl-3-CF_3,[38] 4-Br-3-CF_3,[39] 4-ethoxycarbonyl-phenylhydrazine,[40] and 1-naphthylhydrazine,[40] were prepared according to Enders.[40]

Column chromatography (CC): neutral alumina (Al_2O_3), activity 1 (Merck). Mps: Büchi apparatus, uncorrected. ^{1}H NMR spectra: Varian Gemini-200 spectrometer; $CDCl_3$; δ in ppm rel to Me_4Si as internal standard. *J* in Hz; Ind = hexahydroindolizine, Pip = piperidine, Py = tetrahydropyridine, Pyrr = pyrrolidine, Pz = piperazine, Q = hexahydroquinolizine. Elemental analyses were performed on a *Carlo Erba EA-1110* CHNS-O instrument in the Microanalysis Laboratory of the Department of Pharmaceutical Sciences of Genoa University.

5.2. Aryl/heteroarylazoenamines of structures A, B, C, and D (1–63): general method

To a solution of α-aminoketone (3 mmol) {hexahydro-2H-quinolizin-1-one,[34] hexahydro-8(5H)-indolizinone,[35] 1-Methyl-3-piperidone[36]} in 15 mL of abs. ethanol were added, in the following order, aryl/heteroarylhydrazine hydrochloride (6 mmol) or the corresponding free base, 0.75 mL of conc. hydrochloric acid, and 0.9 mL of 85% phosphoric acid. The mixture was refluxed with stir-

ring for 3 h. After cooling, ethanol was evaporated at reduced pressure, water was added, and the acid solution was basified with 2 M NaOH and extracted with Et_2O. After drying, the solvent was removed obtaining a red-orange oil from which the volatile substances were removed by heating until 80–100 °C under vacuum (0.2 torr). The residue was purified by CC (CH_2Cl_2).

The low (**C**) and high (**D**) melting point isomers, obtained in the reaction with 1-methyl-3-piperidone, were separated by eluting firstly with CH_2Cl_2 and then CH_2Cl_2 + 2%Et_2NH.

In the case of phthalazylazoenamine **23**, the reaction mixture was neutralized and then shaken with CH_2Cl_2 which extracted the compound as hydrochloride.

Compounds **1**–**4**, **6**, **9**, **10**, **13**, **15**, **24**, **26**–**28**, **32**-**35**, **38**, **40**, **44**, **46**, and **51**–**54** have been already described.[2,8,9]

5.2.1. 1-(3-Bromophenylazo)-3,4,6,7,8,9-hexahydro-2*H*-quinolizine (5)

Yield: 42%. Mp 115–117 °C (Et_2O). ^1H NMR ($CDCl_3$): 1.61–1.88 (m, 6H, C(3, 7, 8) of Q); 2.59 (*t*, *J* = 6.5, 2H, C(9) of Q); 3.08–3.36 (m, 6H, C(2, 4, 6) of Q); 7.03–7.63 (m, 4 arom. H). Anal. calcd for $C_{15}H_{18}BrN_3$: C 56.26, H 5.67, N 13.12; found: C 56.45, H 5.69, N 13.09.

5.2.2. 1-(3-Trifluoromethylphenylazo)-3,4,6,7,8,9-hexahydro-2*H*-quinolizine (7)

Yield: 25%. Mp 102–103 °C (Et_2O). ^1H NMR ($CDCl_3$): 1.60–1.97 (m, 6H, C(3, 7, 8) of Q); 2.63 (*t*, *J* = 6.4, 2H, C(9) of Q); 3.07–3.33 (m, 6H, C(2, 4, 6) of Q); 7.22–7.77 (m, 4 arom. H). Anal. calcd for $C_{16}H_{18}F_3N_3$: C 62.13, H 5.87, N 13.58; found: C 62.00, H 6.04, N 13.23.

5.2.3. 1-(3-Nitrophenylazo)-3,4,6,7,8,9-hexahydro-2*H*-quinolizine (8)

Yield: 46%. CC (Et_2O). Mp 132–135°C (Et_2O). ^1H NMR ($CDCl_3$): 1.63–2.00 (m, 6H, C(3, 7, 8) of Q); 2.63 (*t*, *J* = 6.4, 2H, C(9) of Q); 3.12–3.37 (m, 6H, C(2, 4, 6) of Q); 7.30–8.32 (m, 4 arom. H). Anal. calcd for $C_{15}H_{18}N_4O_2$: C 62.92, H 6.34; N 19.57; found: C 62.61, H 6.39, N 19.58.

5.2.4. 1-(3,5-Bis-trifluoromethylphenylazo)-3,4,6,7,8,9-hexahydro-2*H*-quinolizine (11)

Yield: 72%. Mp 147–149 °C (Et_2O). ^1H NMR ($CDCl_3$): 1.64–1.99 (m, 6H, C(3, 7, 8) of Q); 2.63 (*t*, *J* = 6.5, 2H, C(9) of Q); 3.12–3.36 (m, 6H, C(2, 4, 6) of Q); 7.40–7.90 (m, 3 arom. H). Anal. calcd for $C_{17}H_{17}F_6N_3$: C 54,11, H 4.54, N 11.11; found: C 54.00, H 4.72, N 11.02.

5.2.5. 1-(4-Fluoro-3-trifluoromethylphenylazo)-3,4,6,7,8,9-hexahydro-2*H*-quinolizine (12)

Yield: 88%. Mp 133–134 °C (Et_2O). ^1H NMR ($CDCl_3$): 1.60–1.98 (m, 6H, C(3, 7, 8) of Q); 2.58 (*t*, *J* = 6.5, 2H, C(9) of Q); 3.07–3.34 (m, 6H, C(2, 4, 6) of Q); 6.98–7.80 (m, 3 arom. H). Anal. calcd for $C_{16}H_{17}F_4N_3$: C 58.71, H 5.23, N 12.84; found: C 58.51, H 5.43, N 12.59.

5.2.6. 1-(4-Bromo-3-trifluoromethylphenylazo)-3,4,6,7,8,9-hexahydro-2*H*-quinolizine (14)

Yield: 37%. CC (CH_2Cl_2). Mp 155–157 °C (Et_2O). ^1H NMR ($CDCl_3$): 1.62–1.98 (m, 6H, C(3, 7, 8) of Q); 2.60 (*t*, *J* = 6.5, 2H, C(9) of Q); 3.07–3.35 (m, 6H, C(2, 4, 6) of Q); 7.40–7.84 (m, 3 arom. H). Anal. calcd for $C_{16}H_{17}BrF_3N_3$: C 49.50, H 4.41, N 10.82; found: C 49.53, H 4.32, N 10.74.

5.2.7. 1-(1-Naphthylazo)-3,4,6,7,8,9-hexahydro-2*H*-quinolizine (16)

Yield: 58%. CC (CH_2Cl_2). Mp 153–155 °C (Et_2O). ^1H NMR ($CDCl_3$): 1.63–2.00 (m, 6H, C(3, 7, 8) of Q); 2.79 (*t*, *J* = 6.4, 2H, C(9) of Q); 3.15–3.30 (m, 6H, C(2, 4, 6) of Q); 7.32–7.78 (m, 5 arom. H); 8.74–8.84 (m, 1 arom. H). Anal. calcd for $C_{19}H_{21}N_3$: C 78.32, H 7.26, N, 14.42; found: C 78.67, H 7.03, N 14.02.

5.2.8. 1-[4-(7-Chloro)quinolylazo]-3,4,6,7,8,9-hexahydro-2*H*-quinolizine (17)

Yield: 58%. CC (CH_2Cl_2). Mp 203–206 °C (Et_2O). ^1H NMR ($CDCl_3$): 1.74–2.14 (m, 6H, C(3, 7, 8) of Q); 2.89 (*t*, *J* = 6.4, 2H, C(9) of Q); 3.29–3.50 (m, 6H, C(2, 4, 6) of Q); 7.35–8.84 (m, 5 arom. H). Anal. calcd for $C_{18}H_{19}ClN_4$: C 66.15, H 5.86, N 17.14; found: C 66.04, H 6.04, N 17.09.

5.2.9. 8-(4-Chlorophenylazo)-1,2,3,5,6,7-hexahydroindolizine (18)

Yield: 25%. Mp 165–167 °C (Et_2O). ^1H NMR ($CDCl_3$): 1.95–2.20 (m, 4H, C(2, 6) of Ind); 2.65 (*t*, *J* = 6.1, 2H, C(7) of Ind); 3.22 (*t*, *J* = 7.8, 2H, C(1) of Ind); 3.33 (*t*, *J* = 6.0, 2H, C(5) of Ind); 3.55 (*t*, *J* = 6.6, 2H, C(3) of Ind); 7.25 (*d*, *J* = 2.2, 2 arom. H); 7.50 (*d*, *J* = 2.2, 2 arom. H). Anal. calcd for $C_{14}H_{16}ClN_3$: C 64.24, H 6.16, N 16,05: found: C 64.45, H 6.20, N 16.19.

5.2.10. 8-(3-Nitrophenylazo)-1,2,3,5,6,7-hexahydroindolizine (19)

Yield: 43%. Mp 157–159 °C (Et_2O). ^1H NMR ($CDCl_3$): 1.98–2.22 (m, 4H, C(2, 6) of Ind); 2.68 (*t*, *J* = 6.2, 2H, C(7) of Ind); 3.29 (*t*, *J* = 7.9, 2H, C(1) of Ind); 3.38 (*t*, *J* = 6.0, 2H, C(5) of Ind); 3.64 (*t*, *J* = 6.6, 2H, C(3) of Ind); 7.37–8.40 (m, 4 arom. H). Anal. calcd for $C_{14}H_{16}N_4O_2$: C 61.75, H 5.92. N 20.58; found: C 61.78, H 6.04, N 20.45.

5.2.11. 8-(3,4-Dichlorophenylazo)-1,2,3,5,6,7-hexahydroindolizine (20)

Yield: 30%. CC (Et_2O). Mp 176–177 °C (Et_2O). ^1H NMR ($CDCl_3$): 1.87–2.11 (m, 4H, C(2, 6) of Ind); 2.59 (*t*, *J* = 6.4, 2H, C(7) of Ind); 3.17 (*t*, *J* = 7.8, 2H, C(1) of Ind); 3.29 (*t*, *J* = 5.9, 2H, C(5) of Ind); 3.54 (*t*, *J* = 6.6, 2H, C(3) of Ind); 7.18–7.34 (m, 2 arom. H); 7.58 (*d*, *J* = 2.0, 1 arom. H). Anal. calcd for $C_{14}H_{15}Cl_2N_3$: C 56.77, H 5.10, N 14.19; found: C 56.43, H 5.08, N 14.00.

5.2.12. 8-(4-Chloro-3-trifluoromethylphenylazo)-1,2,3,5,6,7-hexahydroindolizine (21)

Yield: 81%. Mp 161–162.5 °C (Et_2O). ^1H NMR ($CDCl_3$): 1.88–2.12 (m, 4H, C(2, 6) of Ind); 2.59 (t, *J* = 6.4, 2H, C(7) of Ind); 3.17 (t, *J* = 7.9, 2H, C(1) of Ind); 3.29 (t, *J* = 5.8, 2H, C(5) of Ind); 3.54 (t, *J* = 7.1, 2H, C(3) of Ind); 7.32 (d, *J* = 8.6, 1 arom. H); 7.56 (dd, *J* = 8.6, 2.0, 1 arom. H); 7.82 (d, *J* = 2.4, 1 arom. H). Anal. calcd for $C_{15}H_{15}ClF_3N_3$: C 54.64, H 4.59, N 12.74; found: C 54.47, H 4.57, N 12.69.

5.2.13. 8-(1-Naphthylazo)-1,2,3,5,6,7-hexahydroindolizine (22)

Yield: 32%. CC (CH_2Cl_2). Mp 148–151 °C (CH_2Cl_2). ^1H NMR ($CDCl_3$): 1.92–2.10 (m, 4H, C(2, 6) of Ind); 2.77 (t, *J* = 6.4, 2H, C(7) of Ind); 3.17–3.30 (m, 4H, C(1, 5) of Ind); 3.46 (t, *J* = 6.9, 2H, C(3) of Ind); 7.33–7.78 (m, 6 arom. H); 8.78–8.85 (m, 1 arom. H). Anal. calcd for $C_{18}H_{19}N_3$: C 77.95, H 6.90, N 15.15; found: C 78.01, H 6.94, 15.13.

5.2.14. 8-(1-Phthalazinylazo)-1,2,3,5,6,7-hexahydroindolizine hydrochloride (23)

Yield: 49%. Mp 174–176 °C (Et_2O). ^1H NMR ($CDCl_3$): 1.90–2.10 (m, 4H, C(2, 6) of Ind); 2.72 (t, *J* = 6.2, 1H, C(7) of Ind); 2.93 (t, *J* = 6.2, 1H, C(7) of Ind); 3.08 (t, *J* = 7.0, 2H, C(1) of Ind); 3.73–3.86 (m, 2H, C(5) of Ind); 4.10–4.28 (m, 2H, C(3) of Ind); 7.88–8.72 (m, 4 arom. H); 9.10 (d, *J* = 8.0, 1 arom. H). Anal. calcd for

$C_{16}H_{17}N_5$ + HCl+H_2O: C 57.57, H 6.04, N 20.97; found: C 57.39, H 6.25, 20.25.

5.2.15. 3-(4-Fluorophenylazo)-1-methyl-1,4,5,6-tetrahydropyridine (25)

Yield: 25%. Mp 82–84 °C (pentane). ^{1}H NMR ($CDCl_3$): 1.98 (q, 2H, C(5) of Py); 2.60 (t, J = 6.4, 2H, C(4) of Py); 3.06 (*s*, CH_3N); 3.22 (t, J = 5.8, 2H, C(6) of Py); 6.97–7.08 (m, 2 arom. H); 7.20 (*s*, 1H, C(2) of Py); 7.49–7.59 (m, 2 arom. H). Anal. calcd for $C_{12}H_{14}FN_3$: C 65.73, H 6.44, N 19.16; found. C 65.52, H 6.15, N 19.28.

5.2.16. 3-(3-Bromophenylazo)-1-methyl-1,4,5,6-tetrahydropyridine (29)

Yield: 20%. Mp 96–99 °C (Et_2O). ^{1}H NMR ($CDCl_3$): 1.99 (q, 2H, C(5) of Py); 2.61 (t, J = 6.4, 2H, C(4) of Py); 3.12 (*s*, CH_3N); 3.26 (t, J = 5.8, 2H, C(6) of Py); 7.20 (*s*, 1H, C(2) of Py); 7.24–7.77 (m, 4 arom. H). Anal. calcd for $C_{12}H_{14}BrN_3$: C 51.44, H 5.04, N 15.00; found: C 51.59, H 5.07, N 14.82.

5.2.17. 3-(4-Bromophenylazo)-1-methyl-1,4,5,6-tetrahydropyridine (30)

Yield: 22%. Mp 112–114 °C (Et_2O). ^{1}H NMR (CDCl3): 1.92 (q, 2H, C(5) of Py); 2.54 (t, J = 6.4, 2H, C(4) of Py); 3.04 (*s*, CH_3N); 3.18 (t, J = 5.8, 2H, C(6) of Py); 7.17 (*s*, 1H, C(2) of Py); 7.34–7.42 (m, 4 arom. H). Anal. calcd for $C_{12}H_{14}BrN_3$: C 51.44, H 5.04, N 15.00; found: C 51. 40, H 4.52, N 14.78.

5.2.18. 1-Methyl-3-(3-trifluoromethylphenylazo)-1,4,5,6-tetrahydropyridine (31)

Yield: 20%. Mp 76–77 °C (pentane). ^{1}H NMR ($CDCl_3$): 1.93 (q, 2H, C(5) of Py); 2.57 (t, J = 6.5, 2H, C(4) of Py); 3.06 (*s*, CH_3N); 3.20 (t, J = 5.8, 2H, C(6) of Py); 7.23 (s, 1H, C(2) of Py); 7.27–7.81 (m, 4 arom. H). Anal. calcd for $C_{13}H_{14}F_3N_3$: C 57.99, H 5.24, N 15.61; found: 57.65, H 5.38, N 15.75.

5.2.19. 3-(3,5-Bis-trifluoromethylphenylazo)-1-methyl-1,4,5,6-tetrahydropyridine (36)

Yield: 20%. Mp 86–87 °C (pentane). ^{1}H NMR ($CDCl_3$): 2.02 (q, 2H, C(5) of Py); 2.64 (t, J = 6.7, 2H, C(4) of Py); 3.18 (s, CH_3N); 3.31 (t, J = 5.8, 2H, C(6) of Py); 7.38 (s, 1H, C(2) of Py); 7.55–8.03 (m, 3 arom. H). Anal. calcd for $C_{14}H_{13}F_6N_3$: C 49.86, H 3.89, N 12.46; found: C 49.91, H 3.60, N 12.30.

5.2.20. 3-(4-Fluoro-3-trifluoromethylphenylazo)-1-methyl-1,4,5,6-tetrahydropyridine (37)

Yield: 30%. Mp 81–84 °C (pentane). ^{1}H NMR ($CDCl_3$): 2.00 (q, 2H, C(5) of Py); 2.61 (t, J = 6.7, 2H, C(4) of Py); 3.13 (s, CH_3N); 3.26 (t, J = 5.9, 2H, C(6) of Py); 7.10–7.87 (m, 1H, C(2) of Py and 3 arom. H). Anal. calcd for $C_{13}H_{13}F_4N_3$: C 54.36, H 4.56, N 14.63; found: C 54.03, H 4.22, N 13.67.

5.2.21. 3-(4-Bromo-3-trifluoromethylphenylazo)-1-methyl-1,4,5,6-tetrahydropyridine (39)

Yield: 34%. Mp 94–95 °C (Et_2O). ^{1}H NMR ($CDCl_3$): 2.01 (q, 2H, C(5) of Py); 2.63 (t, J = 6.4, 2H, C(4) of Py); 3.16 (s, CH_3N); 3.30 (t, J = 5.7, 2H, C(6) of Py); 7.33 (s, 1H, C(2) of Py); 7.59–7.93 (m, 3 arom. H). Anal. calcd for $C_{13}H_{13}BrF_3N_3$: C 44.85, H 3.76, N, 12.07, found: C 44.95, H 4.06 N 11.76.

5.2.22. 1-Methyl-3-pentafluorophenylazo-1,4,5,6-tetrahydropyridine (41)

Yield: 24%. Mp 100–101 °C (pentane). ^{1}H NMR ($CDCl_3$): 1.95 (q, 2H, C(5) of Py); 2.55 (t, J = 6.5, 2H, C(4) of Py); 3.11 (s, CH_3N); 3.25 (t, J = 6.0, 2H, C(6) of Py); 7.27 (s, 1H, C(2) of Py). Anal. calcd for $C_{12}H_{10}F_5N_3$: C 49.49, H 3.46, N 14.43; found: C 49.51, H 3.32, N 14.00.

5.2.23. 1-Methyl-3-(1-naphthylazo)-1,4,5,6-tetrahydropyridine (42)

Yield: 42%. Mp 116–119 °C (Et_2O). ^{1}H NMR ($CDCl_3$): 2.08 (q, 2H, C(5) of Py); 2.82 (t, J = 6.7, 2H, C(4) of Py); 3.14 (s, CH_3N); 3.29 (t, J = 5.7, 2H, C(6) of Py); 7.35 (s, 1H, C(2) of Py); 7.44–7.90 (m, 6 arom. H); 8.79–8.87 (m, 1 arom. H). Anal. calcd for $C_{16}H_{17}N_3$: C 76.46, H 6.82, N 16.72; found: C 76.46, H 6.74, N 16.39.

5.2.24. 1-Benzyl-3-(4-chloro-3-trifluoromethylphenylazo)-1,4,5,6-tetrahydropyridine (43)

Yield: 27%. Mp 118–119 °C (Et_2O). ^{1}H NMR ($CDCl_3$): 1.96 (q, 2H, C(5) of Py); 2.64 (t, J = 5.8, 2H, C(4) of Py); 3.23 (t, J = 5.7, 2H, C(6) of Py); 4.48 (s, 2H, $CH_2C_6H_5$); 7.22–8.02 (m, 8 arom. H and 1H, C(2) of Py). Anal. calcd for $C_{19}H_{17}ClF_3N_3$: C, 60.08, H 4.51, N 11.06; found: C 59.74, H 4.47, N 10.95.

5.2.25. 2-(4-Fluorophenylazo)methylene-1-methylpyrrolidine (45)

Yield: 23%. Mp 107–108 °C (pentane). ^{1}H NMR ($CDCl_3$): 2.07 (q, 2H, C(4) of Pyrr); 2.98 (s, CH_3N); 3.27 (t, J = 7.7, 2H, C(3) of Pyrr); 3.57 (t, J = 7.0, 2H, C(5) of Pyrr); 7.98–8.12 (m, 1H, =CH– and 2 arom. H); 7.50–7.61 (m, 2 arom. H). Anal. calcd for $C_{12}H_{14}FN_3$: C 65.73, H 6.44, N 19.16; found: C 65.60, H 6.12, N 19.31.

5.2.26. 2-(3-Bromophenylazo)methylene-1-methylpyrrolidine (47)

Yield: 22%. Mp 103–107 °C (Et_2O). ^{1}H NMR ($CDCl_3$): 2.08 (q, 2H, C(4) of Pyrr); 3.01 (s, CH_3N); 3.30 (t, J = 7.8, 2H, C(3) of Pyrr); 3.60 (t, J = 7.0, 2H, C(5) of Pyrr); 7.14 (s, 1H, =CH–); 7.20–7.76 (m, 4 arom. H). Anal. calcd for $C_{12}H_{14}BrN_3$: C 51.44, H 5.04, N 15.00; found: C 51.41, H 4.98, N 14.87.

5.2.27. 2-(4-Bromophenylazo)methylene-1-methylpyrrolidine (48)

Yield: 33%. Mp 150–152.5 °C (Et_2O). ^{1}H NMR ($CDCl_3$): 2.02 (q, 2H, C(4) of Pyrr); 2.95 (s, CH_3N); 3.20 (t, J = 7.8, 2H, C(3) of Pyrr); 3.53 (t, J = 7.0, 2H, C(5) of Pyrr); 7.09 (s, 1H, =CH–); 7.34–7.42 (m, 4 arom. H). Anal. calcd for $C_{12}H_{14}BrN_3$: C 51.44, H 5.04, N 15.00; found: C 51.07, H 5.17, N 14.80.

5.2.28. 1-Methyl-2-(3-trifluoromethylphenylazo)methylenepyrrolidine (49)

Yield: 15%. Mp 107–108 °C (Et_2O). ^{1}H NMR ($CDCl_3$): 2.10 (q, 2H, C(4) of Pyrr); 3.03 (s, CH_3N); 3.32 (t, J = 7.9, 2H, C(3) of Pyrr); 3.62 (t, J = 7.0, 2H, C(5) of Pyrr); 7.18 (s, 1H, =CH–); 7.33–7.86 (m, 4 arom. H). Anal. calcd for $C_{13}H_{14}F_3N_3$: C 57.99, H 5.24, N 15.61; found: C 58.11, H 5.55, N 15.33.

5.2.29. 1-Methyl-2-(3-nitrophenylazo)methylenepyrrolidine (50)

Yield: 30%. Mp 117–119 °C (Et_2O). ^{1}H NMR ($CDCl_3$): 2.06 (q, 2H, C(4) of Pyrr); 3.00 (s, CH_3N); 3.27 (t, J = 7.8, 2H, C(3) of Pyrr); 3.60 (t, J = 7.0, 2H, C(5) of Pyrr); 7.18–8.32 (m, 1H, =CH– and 4 arom. H). Anal. calcd For $C_{12}H_{14}N_4O_2$: C 58.53, H 5.73, N 22.75; found: C 58.44, H 5.89, N 22.73.

5.2.30. 1-Methyl-2-(4-nitrophenylazo)methylenepyrrolidine and 1-Methyl-3-(4-nitrophenylazo)-1,4,5,6-tetrahydropyridine (mixture 2:1) (51)

Yield: 60%. Mp 180 °C (EtOH). ^{1}H NMR ($CDCl_3$): 1.98 (q, 0.33 × 2H, C(5) of Py); 2.14 (q, 0.67 × 2H, C(4) of Pyrr); 2.63 (t, J = 6.4, 0.33 × 2H, C(4) of Py); 3.10 (s, 0.67 × 3H, NCH_3 of Pyrr); 3.18 (s, 0.33 × 3H, NCH_3 of Py); 3.22–3.37 (m, 0.67 × 2H, C(3) of

Pyrr) and 0.33 × 2H, C(6) of Py); 3.70 (t, *J* = 7.0, 0.67 × 2H, C(5) of Pyrr); 7.36–7.40 (m, 1H, =CH– of Pyrr and Py); 7.58 (d, *J* = 9.0, 4 arom. H); 8.16 (d, *J* = 9.2, 4 arom. H). Anal. calcd for $C_{12}H_{14}N_4O_2$: C 58.52, H 5.73, N 22.75; found: C 58.75, H 5.72, N 22.87.

5.2.31. 2-(3,5-Bis-trifluoromethylphenylazo)methylene-1-methylpyrrolidine (55)

Yield: 15%. Mp 128–130 °C (Et_2O). ^1H NMR ($CDCl_3$): 2.07(q, 2H, C(4) of Pyrr); 3.01 (s, CH_3N); 3.28 (t, *J* = 7.8, 2H, C(3) of Pyrr); 3.61 (t, *J* = 7.0, 2H, C(5) of Pyrr); 7.19 (s, 1H, =CH–); 7.45–7.70 (m, 3 arom. H). Anal. calcd for $C_{14}H_{13}F_6N_3$: C 49.86, H 3.89, N 12.46; found: C 50.42, H 3.56, N 12.35.

5.2.32. 2-(4-Fluoro-3-trifluoromethylphenylazo)methylene-1-methylpyrrolidine (56)

Yield: 18%. Mp 120–123 °C (Et_2O). ^1H NMR ($CDCl_3$): 2.03 (q, 2H, C(4) of Pyrr); 2.96 (s, CH_3N); 3.23 (t, *J* = 7.8, 2H, C(3) of Pyrr); 3.56 (t, *J* = 7.0, 2H, C(5) of Pyrr); 7.00–7.75 (m, 1H, =CH– and 3 arom. H). Anal. calcd for $C_{13}H_{13}F_4N_3$: C 54.36, H 4.56, N 14.63; found: C 54.34, H 4.56, N 14.60.

5.2.33. 2-(4-Bromo-3-trifluoromethylphenylazo)methylene-1-methylpyrrolidine (57)

Yield: 43%. Mp 126–128 °C (Et_2O). ^1H NMR ($CDCl_3$): 2.12 (q, 2H, C(4) of Pyrr); 3.05 (s, CH_3N); 3.31 (t, *J* = 7.9, 2H, C(3) of Pyrr); 3.65 (t, *J* = 7.1, 2H, C(5) of Pyrr); 7.19 (s, 1H, =CH–); 7.50–7.90 (m, 3 arom. H). Anal. calcd for $C_{13}H_{13}BrF_3N_3$: C 44.85, H 3.76, N 12.07; found: C 44.76, H 3.89, N 11.89.

5.2.34. 1-Methyl-2-(pentafluorophenylazo)methylenepyrrolidine (58)

Yield: 15%. Mp 154–155 °C (pentane). ^1H NMR ($CDCl_3$): 2.10 (q, 2H, C(4) of Pyrr); 3.07 (s, CH_3N); 3.24 (t, *J* = 7.8, 2H, C(3) of Pyrr); 3.67 (t, *J* = 7.1, 2H, C(5) of Pyrr); 7.23 (s, 1H, =CH–). Anal. calcd for $C_{12}H_{10}F_5N_3$: C 49.49, H 3.46, N 14.43; found: C 49.58, H 3.22, N 14.18.

5.2.35. 1-Benzyl-2-phenylazomethylenepyrrolidine (59)

Yield: 43%. Mp 121–123 °C (Et_2O). ^1H NMR ($CDCl_3$): 2.08 (q, 2H, C(4) of Pyrr); 3.38 (t, *J* = 7.7, 2H, C(3) of Pyrr); 3.56 (t, *J* = 7.0, 2H, C(5) of Pyrr); 4.53 (s, 2H, $CH_2C_6H_5$); 7.03–7.73 (m, 1H, =CH– and 10 arom. H). Anal. calcd for $C_{18}H_{19}N_3$: C 77.95, H 6.90, N 15.15; found: C 77,74, H 6.89, N 15.15.

5.2.36. 1-Benzyl-2-(4-chlorophenylazo)methylenepyrrolidine (60)

Yield: 32%. Mp 127–129 °C (EtOH). ^1H NMR ($CDCl_3$): 2.09 (q, 2H, C(4) of Pyrr); 3.37 (t, *J* = 7.8, 2H, C(3) of Pyrr); 3.57 (t, *J* = 7.1, 2H, C(5) of Pyrr); 4.53 (s, 2H, $CH_2C_6H_5$); 6.98–7.76 (m, 1H, =CH– and 9 arom. H). Anal. calcd for $C_{18}H_{18}ClN_3$: C 69.34, H 5.82, N 13.48; found: C 69.02, H 5.78, N 13.40.

5.2.37. 1-Benzyl-2-(4-methylphenylazo)methylenepyrrolidine (61)

Yield: 50%. Mp 122–124 °C (Et_2O). ^1H NMR ($CDCl_3$): 2.07 (q, 2H, C(4) of Pyrr); 2.34 (s, CH_3); 3.37 (t, *J* = 7.6, 2H, C(3) of Pyrr); 3.53 (t, *J* = 7.0, 2H, C(5) of Pyrr); 4.51 (s, 2H, $CH_2C_6H_5$); 7.07–7.63 (m, 1H, =CH– and 9 arom. H). Anal. calcd for $C_{19}H_{21}N_3$: C 78.32, H 7.26, N 14.42; found: C 78.02, H 7.24, N 14.38.

5.2.38. 1-Benzyl-2-(3,4-dichlorophenylazo)methylenepyrrolidine and 1-benzyl-3-(3,4-dichlorophenylazo)-1,4,5,6-tetrahydropyridine (mixture 3:1) (62)

Yield: 57%. Mp 113–115 °C. ^1H NMR ($CDCl_3$): 1.94 (q, 0.25 × 2H, C(5) of Py); 2.10 (q, 0.75 × 2H, C(4) of Pyrr); 2.61 (t, *J* = 6.5, 0.25 × 2H, C(4) of Py); 3.21 (t, *J* = 6.0, 0.25 × 2H, C(6) of Py); 3.38 (t, *J* = 7.7, 0.75 × 2H, C(3) of Pyrr); 3.59 (t, *J* = 7.1, 0.75 × 2H, C(5) of Pyrr); 4.45 (s, 0.25 × 2H, $CH_2C_6H_5$ of Py); 4.54 (s, 0.75 × 2H, $CH_2C_6H_5$ of Pyrr); 7.20–7.70 (m, 1H, =CH– of Pyrr and Py and 8 arom. H). Anal. calcd for $C_{18}H_{17}Cl_2N_3$: C 62.43, H 4.95, N 12.13; found: C 62.68, H 4.96, N 12.16.

5.2.39. 1-Benzyl-2-(4-chloro-3-trifluoromethylphenylazo)-methylenepyrrolidine (63)

Yield: 37%. Mp 114–116 °C (Et_2O). ^1H NMR ($CDCl_3$): 2.12 (q, 2H, C(4) of Pyrr); 3.38 (t, *J* = 7.8, 2H, C(3) of Pyrr); 3.62 (t, *J* = 7.1, 2H, C(5) of Pyrr); 4.47 (s, 2H, $CH_2C_6H_5$); 7.15–7.98 (m, 1H, =CH– and 8 arom. H). Anal. calcd for $C_{19}H_{17}ClF_3N_3$: C 60.08, H 4.51, N 11.06; found: C 59.95, H 4.49, N 10.95.

5.3. 2-(Arylazomethylene)-1,3,3-trimethylindoline (64–65)

The title compounds were prepared through the method used by König and Muller[4] with minor modification. A solution of aniline or 4-chloroaniline (15 mmol) in 6 mL of conc. hydrochloridric acid and 15 mL of water was cooled in an ice bath and a solution of sodium nitrite (15 mmol) in 3.5 mL of cold water was added dropwise. The resulting solution of diazonium salt was then poured slowly into a stirred emulsion of 1,3,3-trimethyl-2-methyleneindoline[41] in 15 mL of water and subsequently added of sodium acetate (10 g). After 1 h at 0 °C with stirring, the aqueous phase was extracted with CH_2Cl_2, the organic phase was dried with sodium sulfate and concentrated to dryness, obtaining, in the case of **64**, an oil which crystallized when treated with the equivalent amount of 1N perchloric acid in abs. ethanol. Compound **65** was a crystalline solid.[32]

5.3.1. 2-(Phenylazomethylene)-1,3,3-trimethylindoline perchlorate (64)

Yield: 64%. Mp 239–240 °C. Anal. calcd for $C_{18}H_{19}N_3$+$HClO_4$: C 57.22, H 5.34, N 11.12; found: C 57.30, H 5.29, N 11.12. Already described as hydroiodide,[3] hydrochloride,[4] and free base,[3,42] which, however, in our hands did not crystallize well.

5.3.2. 2-(4-Chlorophenylazomethylene)-1,3,3-trimethylindoline (65)

Yield: 50%. Mp 132–134 °C (MeOH) lit.[32] 141.5 °C. ^1H NMR ($CDCl_3$): 1.76 (s, 6H, 2 CH_3 of Indoline); 3.35 (s, CH_3N); 6.84–7.33 (m, 5 arom. H); 7.38 (d, *J* = 9.2, 2 arom. H); 7.61 (d, *J* = 9.2, 2 arom. H). Anal. calcd for $C_{18}H_{18}ClN_3$: C 69.33, H 5.82, N 13.48; found: C 69.13, H 5.85, N 13.47.

5.4. 2-Amino-1-arylazoethenes of structure F and G (66–85): general method

a) A solution of the relevant glyoxal monoarylhydrazone (6.75 mmol) and secondary amine (6.5 mmol) in 60 mL of anhydrous toluene was stirred at room temperature for 3 h. After removing the solvent under vacuum, the solid was crystallized with the suitable solvent.
b) The required glyoxal monophenylhydrazone was prepared as described by Severin et al.[5]; in the same way, glyoxal 4-chlorophenylhydrazone[43] and glyoxal 4-ethoxycarbonylphenylhydrazone were prepared. The latter hydrazone is new. Yield: 84%. Mp 163–165 °C (Et_2O). Anal. calcd for $C_{11}H_{12}N_2O_3$: C 59.99, H 5.49, N 12.72; found: C 60.19, H 5.55, N 12.71. ^1H NMR ($CDCl_3$): 1.26 (t, *J* = 7.0, CH_3 of COOEt); 4.25 (q, *J* = 7.0, CH_2 of COOEt); 7.24 (d, *J* = 8.7, 2 arom. H); 7.36 (d, *J* = 9.3, 1H, =CH–); 7.88 (d, *J* = 8.8, 2 arom. H); 9.48 (d, *J* = 10.0, 1H, CHO); 10.97 (s, NH, collapses with D_2O).

Compounds **66** and **69** were already described.[5,6]

5.4.1. 1-(4-Chlorophenylazo)-2-(1-pyrrolidino)ethene (67)

Yield: 41%. Mp 138–140 °C (Et_2O/pentane). ^1H NMR ($CDCl_3$): 1.91–2.08 (m, 4H, C(3, 4) of Pyrr); 3.25–3.57 (m, 4H, C(2, 5) of Pyrr); 7.08 (d, J = 10.8, 1 vinylic H); 7.30 (d, J = 8.7, 2 arom. H); 7.50 (d, J = 8.6, 2 arom. H); 7.66 (d, J = 10.8, 1 vinylic H). Anal. calcd for $C_{12}H_{14}ClN_3$: C 61.15, H 5.99, N 17.83; found: C 60.81, H 5.98, N 17.32.

5.4.2. 1-(4-Carbethoxyphenylazo)-2-(1-pyrrolidino)ethene (68)

Yield: 80%. Mp 163–164 °C (Et_2O). ^1H NMR ($CDCl_3$): 1.37 (t, J = 7.1, CH_3 of COOEt); 1.84–2,10 (m, 4H, C(3, 4) of Pyrr); 3.35–3.54 (m, 4H, C(2, 5) of Pyrr); 4.34 (q, J = 7.0, CH_2 of COOEt); 7.17 (d, J = 10.8, 1 vinylic H); 7.58 (d, J = 8.6, 2 arom. H); 7.71 (d, J = 10.6, 1 vinylic H); 8.02 (d, J = 8.6, 2 arom. H). Anal. calcd for $C_{15}H_{19}N_3O_2$: C 65.91, H 7.01, N 15.37; found: C 66.08, H 7.06, N 15.44.

5.4.3. 1-(4-Carbethoxyphenylazo)-2-(1-piperidino)ethene (70)

Yield: 63%. Mp 122–124 °C (Et_2O). ^1H NMR ($CDCl_3$): 1.37 (t, J = 7.1, CH_3 of COOEt); 1.60–1.74 (m, 6H, C(3, 4, 5) of Pip); 3.30–3.44 (m, 4H, C(2, 6) of Pip); 4.34 (q, J = 7.0, CH_2 of COOEt); 7.30–7.50 (m, 2 vinylic H); 7.58 (d, J = 8.8, 2 arom. H); 8.03 (d, J = 8.8, 2 arom. H). Anal. calcd for $C_{16}H_{21}N_3O_2$: C 66.88, H 7.37, N 14.62; found: C 66.60, H 7.27, N 14.59.

5.4.4. 2-(4-Morpholino)-1-phenylazoethene (71)

Yield: 54%. Mp 106 °C (Et_2O). ^1H NMR ($CDCl_3$): 3.37 (t, J = 4.9, 4H, morpholine); 3.78 (t, J = 4.9, 4H, morpholine); 7.15 (d, J = 11.0, 1 vinylic H); 7.35–7.70 (m, 5 arom. H and 1 vinylic H). Anal. calcd for $C_{12}H_{15}N_3O$: C 66.34, H 6.96, N 19.34; found: C 66.03, H 6.85, N 19.25.

5.4.5. 1-Phenylazo-2-(4-thiomorpholino)ethene (72)

Yield: 48%. Mp 88–89 °C (Et_2O). ^1H NMR ($CDCl_3$): 2.76 (t, J = 5.0, 4H, thiomorpholine); 3.70 (t, J = 5.1, 4H, thiomorpholine); 7.10–7.70 (m, 5 arom. H and 2 vinylic H). Anal. calcd for $C_{12}H_{15}N_3S$: C 61.77, H 6.48, N 18.01, S 13.74; found: C 61.47, H 6.46, N 18.35, S 13.43.

5.4.6. 2-[(4-Ethoxycarbonyl)piperazin-1-yl]-1-phenylazoethene (73)

Yield: 53%. Mp 106–107 °C (CH_2Cl_2/Et_2O). ^1H NMR ($CDCl_3$): 1.29 (t, J = 7.1, CH_3 of COOEt); 3.35 (t, J = 5.2, 4H, C(3, 5) of Pz); 3.60 (t, J = 5.1, 4H, C(2, 6) of Pz); 4.18 (q, J = 7.1, CH_2 of COOEt); 7.11–7.66 (m, 5 arom. H and 2 vinylic H). Anal. calcd for $C_{15}H_{20}N_4O_2$: C 62.48, H 6.99, N 19.43; found: C 62.47, H 7.00, N 19.53.

5.4.7. 1-Phenylazo-2-[4-(pyridin-2-yl)piperazin-1-yl]ethene (74)

Yield: 75%. Mp 114–116 °C (CH_2Cl_2/Et_2O). ^1H NMR ($CDCl_3$): 3.50 (t, J = 5.1, 4H, C(3, 5) of Pz); 3.71 (t, J = 5.2, 4H, C(2, 6) of Pz); 6.65–7.65 (m, 5 arom. H, 2 vinylic H and 3H, C(3, 4, 5) of Pyridine); 8.20–8.26 (m, 1H, C(6) of Pyridine). Anal. calcd for $C_{17}H_{19}N_5$: C 69.60, H 6.53, N 23.87; found: 69.62, H 6.57, N 24.01.

5.4.8. 1-Phenylazo-2-[4-(pyrimidin-2-yl)piperazin-1-yl]ethene (75)

Yield: 74%. Mp 140–142 °C (CH_2Cl_2/Et_2O). ^1H NMR ($CDCl_3$): 3.46 (t, J = 5.2, 4H, C(3, 5) of Pz); 3.98 (t, J = 5.3, 4H, C(2, 6) of Pz); 6.57 (t, J = 5.0, 1H, C(5) of Pyrimidine); 7.20–7.65 (m, 5 arom. H and 2 vinylic H); 8.35 (d, J = 4.9, 2H, C(4, 6) of Pyrimidine). Anal. calcd for $C_{16}H_{18}N_6$: C 65.29, H 6.16, N 28.55; found: C 65.01, H 6.14, N 28.79.

5.4.9. 1-Phenylazo-2-(4-phenylpiperazin-1-yl)ethene (76)

Yield: 77%. Mp 159–161 °C (CH_2Cl_2/Et_2O). ^1H NMR ($CDCl_3$): 3.29 (t, J = 5.4, 4H, C(3, 5) of Pz); 3.54 (t, J = 5.5, 4H, C(2, 6) of Pz); 6.90–7.67 (m, 10 arom. H and 2 vinylic H). Anal. calcd for $C_{18}H_{20}N_4$: C 73.94, H 6.89, N 19.16; found: C 73.64, H 6.97, N 19.40.

5.4.10. 2-[4-(2-Fluorophenyl)piperazin-1-yl]-1-phenylazoethene (77)

Yield: 68%. Mp 129–131 °C (CH_2Cl_2/Et_2O). ^1H NMR ($CDCl_3$): 3.16 (t, J = 5.0, 4H, C(3, 5) of Pz); 3.54 (t, J = 5.0, 4H, C(2, 6) of Pz); 6.85–7.66 (m, 9 arom. H and 2 vinylic H). Anal. calcd for $C_{18}H_{19}FN_4$: C 69.66, H 6.17, N 18.05; found: C 69.24, H 5.98, N 17.85.

5.4.11. 2-[4-(4-Fluorophenyl)piperazin-1-yl]-1-phenylazoethene (78)

Yield: 68%. Mp 168–170 °C (toluene). ^1H NMR ($CDCl_3$): 3.17 (t, J = 5.0, 4H, C(3, 5) of Pz); 3.51 (t, J = 5.2, 4H, C(2, 6) of Pz); 6.85–7.66 (m, 9 arom. H and 2 vinylic H). Anal. calcd for $C_{18}H_{19}FN_4 + 0.5\ H_2O$: C 67.69, H 6.31, N 17.54; found: C 67.82, H 6.14, N 17.82.

5.4.12. 2-[4-(2-Chlorophenyl)piperazin-1-yl]-1-phenylazoethene (79)

Yield: 49%. Mp 83–85 °C (CH_2Cl_2/Et_2O). ^1H NMR (CDCl3): 3.13 (t, J = 4.8, 4H, C(3, 5) of Pz); 3.55 (t, J = 4.9, 4H, C(2, 6) of Pz); 6.97–7.65 (m, 9 arom. H and 2 vinylic H). Anal. calcd for $C_{18}H_{19}ClN_4$: C 66.15, H 5.86, N 17.14; found: 66.00, H 5.96, N 17.30.

5.4.13. 2-[4-(3-Chlorophenyl)piperazin-1-yl]-1-phenylazoethene (80)

Yield: 75%. Mp 134–135 °C (CH_2Cl_2/Et_2O). ^1H NMR ($CDCl_3$): 3.27 (t, J = 5.1, 4H, C(3, 5) of Pz); 3.50 (t, J = 5.2, 4H, C(2, 6) of Pz); 6.76–7.63 (m, 9 arom. H and 2 vinylic H). Anal. calcd for $C_{18}H_{19}ClN_4$: C 66.15, H 5.86, N 17.14; found: 66.19, H 5.92, N 17.28.

5.4.14. 2-[4-(4-Chlorophenyl)piperazin-1-yl]-1-phenylazoethene (81)

Yield: 87%. Mp 197–198 °C (toluene). ^1H NMR ($CDCl_3$): 3.22 (t, J = 5.1, 4H, C(3, 5) of Pz); 3.51 (t, J = 5.2, 4H, C(2, 6) of Pz); 6.80–7.65 (m, 9 arom. H and 2 vinylic H). Anal. calcd for $C_{18}H_{19}ClN_4$: C 66.15, H 5.86, N 17.14; found: 65.84, H 6.00, N 17.39.

5.4.15. 1-Phenylazo-2-[4-(3-trifluoromethylphenyl)piperazin-1-yl]ethene (82)

Yield: 69%. Mp 146–148 °C (CH_2Cl_2/Et_2O). ^1H NMR ($CDCl_3$): 3.32 (t, J = 5.1, 4H, C(3, 5) of Pz); 3.53 (t, J = 5.2, 4H, C(2, 6) of Pz); 7.04–7.64 (m, 9 arom. H and 2 vinylic H). Anal. calcd for $C_{19}H_{19}F_3N_4$: C 63.32, H 5.31, N 15.55; found: C 63.06, H 5.39, N 15.91.

5.4.16. 2-[4-(4-Nitrophenyl)piperazin-1-yl]-1-phenylazoethene (83)

Yield: 90%. Mp 215–217 °C (CH_2Cl_2/Et_2O). ^1H NMR ($CDCl_3$): 3.50–3.61 (m, 8H, C(2, 3, 5, 6) of Pz); 6.86 (d, J = 9.4, 2 arom. H, p-NO_2-phenyl); 7.18–7.65 (m, 5 arom. H and 2 vinylic H); 8.17 (d, J = 9.4, 2 arom. H, p-NO_2-phenyl). Anal. calcd for $C_{18}H_{19}N_5O_2$: C 64.08, H 5.68, N 20.76; found: C 64.01, H 5.71, N 20.55.

5.4.17. 2-[4-(4-Acetylphenyl)piperazin-1-yl]-1-phenylazoethene (84)

Yield: 79%. Mp 188–190 °C (toluene). ^1H NMR ($CDCl_3$): 2.55 (s, CH_3CO); 3.45–3.60 (m, 8H, C(2, 3, 5, 6) of Pz); 6.86 (d, J = 9.4, 2 arom. H, p-NO_2-phenyl); 7.18–7.65 (m, 5 arom. H and 2 vinylic H); 8.17 (d, J = 9.4, 2 arom. H, p-NO_2-phenyl). Anal. calcd for $C_{20}H_{22}N_4O + 0.5H_2O$: C 69.64, H 6.75, N 16.31; found: C 70.34, H 6.58, N 16.28.

5.4.18. 2-[4-(4-Methoxyphenyl)piperazin-1-yl]-1-phenylazoethene (85)

Yield: 60%. Mp 173–175 °C (toluene). ^1H NMR ($CDCl_3$): 3.16 (t, J = 5.0, 4H, C(3, 5) of Pz); 3.53 (t, J = 5.1, 4H, C(2, 6) of Pz); 3.79 (s, CH_3O); 6.97–7.65 (m, 9 arom. H and 2 vinylic H). Anal. calcd for $C_{19}H_{22}N_4O$: C 70.78, H 6.88, N 17.38; found: C 70.51, H 6.81, N 17.39.

5.5. Cell-based assays

5.5.1. Compounds

Compounds were dissolved in DMSO at 100 mM and then diluted in culture medium.

5.5.2. Cells and viruses

Cell lines were purchased from American Type Culture Collection (ATCC). The absence of mycoplasma contamination was checked periodically by the Hoechst staining method. Cell lines supporting the multiplication of RNA and DNA viruses were the following: $CD4^+$ human T cells containing an integrated HTLV-1 genome (MT-4); Madin Darby bovine kidney (MDBK); baby hamster kidney (BHK-21) and monkey kidney (Vero-76) cells.

5.5.3. Cytotoxicity assays

For cytotoxicity tests, run in parallel with antiviral assays, MDBK and BHK cells were resuspended in 96 multiwell plates at an initial density of 6×10^5 and 1×10^6 cells/mL, respectively, in maintenance medium, without or with serial dilutions of test compounds. Cell viability was determined after 48–96 h at 37 °C in a humidified CO_2 (5%) atmosphere by the 3-(4,5-dimethylthiazol-2-yl)-2,5-diphenyl-tetrazolium bromide (MTT) method.[44] Vero-76 cells were resuspended in 24 multiwell plates at an initial density of 4×10^5 cells/mL. The cell number of Vero-76 monolayers was determined by staining with the crystal violet dye.

For cytotoxicity evaluations, exponentially growing cells derived from human hematological tumors [$CD4^+$ human T-cells containing an integrated HTLV-1 genome (MT-4)] were seeded at an initial density of 1×10^5 cells/mL in 96-well plates in RPMI-1640 medium supplemented with 10% fetal calf serum (FCS), 100 U/mL penicillin G and 100 μg/ml streptomycin. Cell cultures were then incubated at 37 °C in a humidified, 5% CO_2 atmosphere in the absence or presence of serial dilutions of test compounds. Cell viability was determined after 96 h at 37 °C by the MTT method.

5.5.4. Antiviral assay

Activity of compounds against human immunodeficiency virus type-1 (HIV-1) was based on inhibition of virus-induced cytopathogenicity in MT-4 cells acutely infected with a multiplicity of infection (m.o.i.) of 0.01. Briefly, 50 μL of RPMI containing 1×10^4 MT-4 were added to each well of flat-bottom microtitre trays containing 50 μL of RPMI, without or with serial dilutions of test compounds. Then, 20 μL of a HIV-1 suspension containing 100 $CCID_{50}$ were added. After a 4-day incubation, cell viability was determined by the MTT method.

Activity of compounds against yellow fever virus (YFV) and Reo virus type-1 (Reo-1) was based on inhibition of virus-induced cytopathogenicity in acutely infected BHK-21 cells. Activities against bovine viral diarrhoea virus (BVDV), in infected MDBK cells, were also based on inhibition of virus-induced cytopathogenicity.

BHK and MDBK cells were seeded in 96-well plates at a density of 5×10^4 and 3×10^4 cells/well, respectively, and were allowed to form confluent monolayers by incubating overnight in growth medium at 37 °C in a humidified CO_2 (5%) atmosphere. Cell monolayers were then infected with 50 μL of a proper virus dilution (in serum-free medium) to give a m.o.i = 0.01. One hour later, 50 μL of MEM Earle's medium, supplemented with inactivated fetal calf serum (FCS), 1% final concentration, without or with serial dilutions of test compounds, were added. After 3–4 days of incubation at 37 °C, cell viability was determined by the MTT method.

Activity of compounds against coxsackie virus type B2 (CVB-2), Polio Virus type-1 Sabin strain (Sb-1), vesicular stomatitis virus (VSV), vaccinia virus (VV), herpes virus 1 (HSV-1) and respiratory syncytial virus (RSV), A-2 strain, in infected Vero-76 cells, was determined by plaque reduction assays in Vero-76 cell monolayers. To this end, Vero-76 cells were seeded in 24-well plates at a density of 2×10^5 cells/well and were allowed to form confluent monolayers by incubating overnight in growth medium at 37 °C in a humidified CO_2 (5%) atmosphere. Then, monolayers were infected with 250 μL of proper virus dilutions to give 50–100 PFU/well. Following removal of unadsorbed virus, 500 μL of Dulbecco's modified Eagle's medium supplemented with 1% inactivated FCS and 0.75% methyl-cellulose, without or with serial dilutions of test compounds, were added. Cultures were incubated at 37 °C for 2 (Sb-1 and VSV), 3 (CVB-2, VV and HSV-1) or 5 days (RSV) and then fixed with PBS containing 50% ethanol and 0.8% crystal violet, washed and air-dried. Plaques were then counted. EC_{50} (50% effective concentration) was calculated by linear regression technique.

5.6. Molecular modeling

5.6.1. Pharmacophore modeling

The model structures of all compounds were built using the *CATALYST* 2D–3D sketcher,[45] and the conformational search of each compound was carried out using the Poling algorithm[46–48] and generalized CHARMM force field[49] as implemented in the program. Molecular flexibility was taking into account by considering each compound as a collection of conformers representing a different area of conformational space accessible to the molecule within a given energy range. The 'best quality' generation option was adopted to select representative conformers over a 0–20 kcal/mol interval above the computed global energy minimum in the conformational space. Since the number of conformers generated for each compound has been limited to a maximum of 250, this search procedure should identify the best three-dimensional arrangement of chemical functions explaining the activity variations among the compound training set.

Based on the conformations for each compound, *CATALYST* 4.9 software package was used to generate plausible three-dimensional pharmacophore models. During hypotheses generation, the software attempts to minimize a cost function of two main terms: the first penalizes the deviation between the estimated activities of the training set molecules and their experimental values, while the second penalizes the complexity of the hypothesis. The uncertain factor for each compound represents the ratio range of uncertainty in the activity value based on the expected statistical straggling of biological data collection. Uncertainty influences the first step—also called the constructive phase—of the hypothesis generating process.[50] In this work, an uncertainty of 2.0 was preferred over the default factor of 3.0, as the experimental activities of our compounds barely span the required four orders of magnitude.

An analysis of the functional groups characterizing our compounds suggested that hydrophobic aromatic (HAr) sites, hydrogen bond acceptors (HBA), hydrogen bond donors (HBD), positive ionizable points (PI), and ring aromatic (RAr) sites could effectively map their critical chemical features and, hence, describe the antiviral activity of our compounds. Accordingly, these five features were selected to constitute the essential information in the automated hypothesis generation process.

Two validation procedures were followed to determine the statistical relevance and the validity of the proposed 3D pharmacophore models: the test set prediction model, and the *Cat-Scramble* method. In this work, the former procedure consisted in the collection of further, different compounds into three sets (TsS), and in performing a regression analysis by mapping each TsS onto the best pharmacophore hypothesis for each virus. The obtainment of high correlation coefficients generated using the test set compounds revealed the good correlation between the actual and estimated activities and, hence, the predictive validity of the corresponding 3D hypothesis. The *Cat-Scramble* validation procedure is based on Fisher's randomization test.[51] The goal of this

type of validation is to check whether there is a strong correlation between the chemical structures and the biological activity. This is done by randomizing the activity data associated with the training set compounds, generating pharmacophore hypothesis using the same features and parameters employed to develop the original pharmacophore model. The statistical significance is calculated according to the following formula:

$$\text{significance} = 100 \times [1 - (1 + x/y)]$$

where x is the total number of hypotheses having a total cost lower than the original (best) hypothesis, and y is the total number of *HypoGen* runs (initial + random runs). Thus, for instance, 49 random spreadsheets (i.e., 49 *HypoGen* runs) have to be generated to obtain a 98% confidence level. Should any randomized data set result in the generation of a 3D pharmacophore with similar or even better cost values, root-mean-square deviations, and correlation coefficients, then it is likely that the original hypothesis does reflect a chance correlation.

Acknowledgments

Financial support from Italian MIUR (FIRB RBNE01J3SK01) is gratefully acknowledged. The authors thank O. Gagliardo for performing elemental analyses.

References and notes

1. Sparatore, F.; Boido, V. *Farmaco* **1988**, *43*, 1099.
2. Boido Canu, C.; Boido, V.; Sparatore, F.; Sparatore, A.; Susanna, V.; Russo, S.; Cenicola, M. L.; Marmo, E. *Farmaco, Ed. Sci.* **1988**, *43*, 819.
3. Rosenhauer, E. *Chem. Ber.* **1924**, *57*, 1192.
4. König, W.; Müller, J. *Chem. Ber.* **1924**, *57*, 144.
5. Severin, T.; Adam, R.; Lerche, H. *Chem. Ber.* **1975**, *108*, 1756.
6. Lerche, H.; Severin, T. *Chem. Ber.* **1978**, *111*, 1195.
7. Crary, J. W.; Quayle, O. R.; Lester, C. T. *J. Am. Chem. Soc.* **1956**, *78*, 5584.
8. Sparatore, A.; Canu Boido, C.; Boido, V.; Sparatore, F.; Debbia, E.; Pesce Schito, A. *Farmaco* **1990**, *45*, 867.
9. Canu Boido, C.; Boido, V.; Sparatore, F.; Sparatore, A.; Bombieri, G.; Benetollo, F.; Debbia, E.; Pesce Schito, A. *Farmaco* **1993**, *48*, 749.
10. Elslager, E. F.; Worth, D. F. *J. Med. Chem.* **1963**, *6*, 444.
11. Elslager, E. F.; Capps, D. B.; Kurz, D. H.; Short, F. W.; Werbel, L. M.; Worth, D. F. *J. Med. Chem.* **1966**, *9*, 378.
12. Werbel, L. M.; Elslager, E. F.; Fisher, M. W.; Gavrilis, Z. B.; Phillips, A. A. *J. Med. Chem.* **1968**, *11*, 411.
13. Vazzana, I.; Sparatore, F.; Fadda, G.; Manca, C. *Farmaco* **1993**, *48*, 737.
14. Milhavet, O.; Mange, A.; Casanova, D.; Lehmann, S. *J. Neurochem.* **2000**, *74*, 222.
15. Corsaro, A.; Paludi, D.; Villa, V.; D'Arrigo, C.; Chiovitti, K.; Thellung, S.; Russo, C.; Di Cola, D.; Ballerini, P.; Patrone, E.; Schettini, G.; Aceto, A.; Florio, T. *Int. J. Immunopathol. Pharmacol.* **2006**, *19*, 339. and references reported therein.
16. Kimball, D. B.; Haley, M. M. *Angew. Chem. Int. Ed.* **2002**, *41*, 3338.
17. Gesher, J. A.; Hickman, J. A.; Simmonds, R. J.; Stevens, M. F. G.; Vaughan, K. *Biochem. Pharmacol.* **1981**, *30*, 89.
18. Stevens, M. F. G.; Phillip, K. S.; Rathbone, D. L.; O'Shea, D. M.; Queener, S. F.; Schwalbe, C. H.; Lambert, P. A. *J. Med. Chem.* **1997**, *40*, 1886.
19. Prous, J.; Graul, A.; Castañer, J. *Drugs Future* **1994**, *19*, 746.
20. Jean-Claude, B. J.; Just, G. *J. Chem. Soc. Perkin Trans. I* **1991**, 2525.
21. Jean-Claude, B. J.; Just, G. *Heterocycles* **1998**, *48*, 1347.
22. Jean-Claude, B. J.; Mustafa, A.; Damian, Z.; De Marte, J.; Vasilescu, D. E.; Yen, R.; Chan, T. H.; Leyland-Jones, B. *Biochem. Pharmacol.* **1999**, *288*, 753.
23. Jean-Claude, B. J.; Mustafa, A.; Watson, A. J.; Damian, Z.; Vasilescu, D.; Chan, T. H.; Leyland-Jones, B. *J. Pharmacol. Exp. Ther.* **1999**, *288*, 484.
24. Dumont-Hornebeck, B.; Strube, Y. N.; Vasilescu, D.; Jean-Claude, B. J. *Bioorg. Med. Chem. Lett.* **2000**, *10*, 2325.
25. Miyadera, T. In *The Chemistry of Hydrazo, Azo and Azoxy Groups*; Patai, S., Ed.; J. Wiley: London, New York, 2002; pp 495–539.
26. Polanc, S. *J. Heterocyclic Chem.* **2005**, *42*, 401.
27. Reich, M. F.; Fabio, P. F.; Lee, V. J.; Kuck, N. A.; Testa, R. T. *J. Med. Chem.* **1989**, *32*, 2474.
28. Barbieri, F.; Sparatore, A.; Alama, A.; Novelli, F.; Bruzzo, C.; Sparatore, F. *Oncol. Res.* **2003**, *13*, 455.
29. Sparatore, F.; Cerri, R. *J. Heterocyclic Chem.* **1979**, *16*, 1001.
30. Sparatore, F.; Boido, A. *Farmaco* **1991**, *46*(Suppl.), 233.
31. Novelli, F.; Sparatore, F. *Farmaco* **2002**, *57*, 871.
32. Gault, F.; Wahl, H. *Compt. Rend.* **1955**, *240*, 983.
33. Sommer, S. *Angew. Chem. Int. Ed.* **1977**, *16*, 58.
34. Reckhow, W. A.; Tarbell, D. S. *J. Am. Chem. Soc.* **1952**, *74*, 4960.
35. Kunieda, T.; Koga, K.; Yamada, S.-I. *Chem. Pharm. Bull.* **1967**, *15*, 337.
36. Hirsch, J. A.; Jarmas, A. A. *J. Org. Chem.* **1978**, *43*, 4106.
37. Haylor, B. D. G.; Smith, P. H. G. Eur. Pat. Appl. EP 634,413, 1995; *Chem. Abstr.* **1995**, *122*, 214088.
38. Nagarajan, K.; Talwalker, P. K.; Kulkarni, C. L.; Venkateswarlu, A.; Prabhu, S. S.; Nayak, G. V. *Ind. J. Chem. Sect. B* **1984**, *23B*, 1243.
39. Challand, S. R.; Copp, F. C.; Denyer, C. V.; Eakins, K. E.; Walker, J. M. G.; Whittaker, N.; Caldwell, A. G. Eur. Pat. Appl. EP 22,578, 1981; *Chem. Abstr.* **1981**, *95*, 62193.
40. Enders, E. In *Houben-Weyl*; Müller, E., Ed.; Methoden der organischen Chemie; G. Thieme Verlag: Stuttgart, 1967; Vol. 10/II, pp 201–214.
41. Plancher, G. *Gazz. Chim. It.* **1898**, *28 II*, 418.
42. Colonna, M.; Bruni, P. *Gazz. Chim. It.* **1965**, *95*, 857.
43. Clark, J. D.; Heise, J. D.; Shah, A. S.; Peterson, J. C.; Chou, S. K.; Levine, J.; Karakas, A. M.; Ma, Y.; Ng, K.-Y.; Patelis, L.; Springer, J. R.; Stano, D. R.; Wettach, R. H.; Dutra, G. A. *Org. Proc. Res. Dev.* **2004**, *8*, 176.
44. Pauwels, R.; Balzarini, J.; Baba, M.; Snoeck, R.; Schols, D.; Herdewijn, P.; Desmyster, J.; De Clercq, E. *J. Virol. Methods* **1988**, *20*, 309.
45. *CATALYST* 4.9; Accelrys Inc., San Diego, CA, USA, 2004.
46. Smellie, A.; Teig, S. L.; Towbin, P. *J. Comput. Chem.* **1994**, *16*, 171.
47. Smelie, A.; Kahn, S. D.; Teig, S. L. *J. Chem. Inf. Comput. Sci.* **1995**, *35*, 285.
48. Smelie, A.; Kahn, S. D.; Teig, S. L. *J. Chem. Inf. Comput. Sci.* **1995**, *35*, 295.
49. Brooks, B. R.; Bruccoleri, R. E.; Olafson, B. D.; States, D. J.; Swaminathan, S.; Karplus, M. J. *J. Comput. Chem.* **1983**, *4*, 187.
50. Güner, O. F. In *Pharmacophore Perception Development and Use in Drug Design*; International University Line: La Jolla, CA, USA, 2000; p 173.
51. Fisher, R. *The Design of Experiments*; Hafner Publishing: New York, NY, USA, 1966.